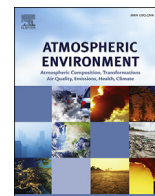




Contents lists available at ScienceDirect

Atmospheric Environment

journal homepage: www.elsevier.com/locate/atmosenv

Application of Weather Research and Forecasting Model with Chemistry (WRF/Chem) over northern China: Sensitivity study, comparative evaluation, and policy implications

Litao Wang^{a, b, *}, Yang Zhang^{b, c}, Kai Wang^b, Bo Zheng^d, Qiang Zhang^d, Wei Wei^e^a Department of Environmental Engineering, Hebei University of Engineering, Handan, Hebei 056038, China^b Department of Marine, Earth and Atmospheric Science, North Carolina State University, Raleigh, NC 27695, USA^c State Key Joint Laboratory of Environment Simulation and Pollution Control, School of Environment, Tsinghua University, Beijing 100084, China^d Center for Earth System Science, Tsinghua University, Beijing 100084, China^e Department of Environmental Science, Beijing University of Technology, Beijing 100124, China

HIGHLIGHTS

- WRF/Chem is applied for the most polluted month over northern China.
- The optimal set of configurations with the best performance is identified.
- PM_{2.5} sensitivities to emission reductions are quantified.

ARTICLE INFO

Article history:

Received 29 June 2014

Received in revised form

18 December 2014

Accepted 19 December 2014

Available online 20 December 2014

Keywords:

WRF/Chem

PM_{2.5}

Regional haze

Northern China

Comparative evaluation

Sensitivity study

ABSTRACT

An extremely severe and persistent haze event occurred over the middle and eastern China in January 2013, with the record-breaking high concentrations of fine particulate matter (PM_{2.5}). In this study, an online-coupled meteorology-air quality model, the Weather Research and Forecasting Model with Chemistry (WRF/Chem), is applied to simulate this pollution episode over East Asia and northern China at 36- and 12-km grid resolutions. A number of simulations are conducted to examine the sensitivities of the model predictions to various physical schemes. The results show that all simulations give similar predictions for temperature, wind speed, wind direction, and humidity, but large variations exist in the prediction for precipitation. The concentrations of PM_{2.5}, particulate matter with aerodynamic diameter of 10 μm or less (PM₁₀), sulfur dioxide (SO₂), and nitrogen dioxide (NO₂) are overpredicted partially due to the lack of wet scavenging by the chemistry-aerosol option with the 1999 version of the Statewide Air Pollution Research Center (SAPRC-99) mechanism with the Model for Simulating Aerosol Interactions and Chemistry (MOSAIC) and the Volatility Basis Set (VBS) for secondary organic aerosol formation. The optimal set of configurations with the best performance is the simulation with the Goddard shortwave and RRTM longwave radiation schemes, the Purdue Lin microphysics scheme, the Kain-Fritsch cumulus scheme, and a nudging coefficient of 1×10^{-5} for water vapor mixing ratio. The emission sensitivity simulations show that the PM_{2.5} concentrations are most sensitive to nitrogen oxide (NO_x) and SO₂ emissions in northern China, but to NO_x and ammonia (NH₃) emissions in southern China. 30% NO_x emission reductions may result in an increase in PM_{2.5} concentrations in northern China because of the NH₃-rich and volatile organic compound (VOC) limited conditions over this area. VOC emission reductions will lead to a decrease in PM_{2.5} concentrations in eastern China. However, 30% reductions in the emissions of SO₂, NO_x, NH₃, and VOC, individually or collectively, are insufficient to effectively mitigate the severe pollution over northern China. More aggressive emission controls, which needs to be identified in further studies, are needed in this area to reach the objective of 25% PM_{2.5} concentration reduction in 2017 proposed in the Action Plan for Air Pollution Prevention and Control by the State Council in 2013.

© 2014 Elsevier Ltd. All rights reserved.

* Corresponding author. Department of Environmental Engineering, Hebei University of Engineering, Handan, Hebei 056038, China.

E-mail address: wanglitao@hebeu.edu.cn (L. Wang).

1. Introduction

Since January 2013, very frequent and severe haze events occurred over central and eastern China, with the record-breaking high concentrations of fine particulate matter (PM_{2.5}) in many cities. Haze has emerged as the most urgent air pollution problem that needs to be addressed in China, more than other existing issues, e.g., photochemical pollution or acid rain. The extremely severe pollution over northern China that covers Beijing-Tianjin-Hebei area (BTH), Shanxi, Henan, and Shandong, has raised widespread public concerns. According to the monthly report publicized by the Ministry of Environmental Protection (MEP) on the top ten polluted cities in China, seven of the nine top polluted cities are within the BTH area (<http://www.mep.gov.cn/zhxx/xwfb/>). There is an urgent need of understanding the sources and formation mechanisms of the severe haze occurred over this area.

The pollution characteristics and source apportionment over China using 3-D air quality models have been increasingly studied in the past few decades. For example, many studies have been performed to support the policy-making for the 2008 Beijing Olympics and the National Five Year Plan (FYP) using the Community Multiscale Air Quality Model (CMAQ) system (Streets et al., 2007; Chen et al., 2007, 2008; Wang et al., 2008, 2009, 2011; Fu et al., 2009; Zhou et al., 2010, 2012; Xing et al., 2011; Gao and Zhang, 2012; Li et al., 2013; Zhao et al., 2013). However, all those studies used an offline-coupled meteorology and air quality model system, i.e., the meteorological model is run separately from the air quality model to provide the meteorological fields (Zhang, 2008; Zhang et al., 2012a). It does not simulate the feedbacks of chemistry to meteorology, such as the aerosol feedbacks to radiation and photolysis, which may be very important during severe pollution periods with high aerosol loading (J. D. Wang et al., 2014a). January 2013 has been reported as the haziest month in the past 60 years in Beijing (Lu et al., 2013), and the haziest month since this century in northern China (L. T. Wang et al., 2014b). This month is representative for understanding the severe haze and PM_{2.5} pollution episodes frequently occurred in recent years over northern China. Several recent studies focus on this month in terms of the pollution characteristics, formation mechanism, chemical and physical processes, and source apportionment (Ji et al., 2014; Jiang et al., 2014; L. T. Wang et al., 2014b; J. D. Wang et al., 2014a; Zheng et al., 2014; Y. S. Wang et al., 2014c). The results of J. D. Wang et al. (2014a), using the coupled Weather Research and Forecasting (WRF)-CMAQ system, shows that during that month the aerosol-meteorology feedbacks can lead to a maximum 53% reduction in incoming radiation and as high as 140 µg m⁻³ increase in PM_{2.5} concentrations on daily average in Beijing. It is therefore necessary to apply the online-coupled meteorology-air quality model to simulate the extremely severe haze episodes over this area and understand the underlying formation mechanisms.

The Weather Research and Forecasting Model with Chemistry (WRF/Chem) (Grell et al., 2005; Fast et al., 2006) is one of the most advanced online-coupled 3-D air quality models, which has been increasingly applied at global, continental, and regional scales over North America, Europe, and Asia in recent years (Misenis and Zhang, 2010; Zhang et al., 2010a, 2012b, c; 2013; Tuccella et al., 2012; Situ et al., 2013; Tie et al., 2009, 2013; Chen et al., 2013; Wu et al., 2013). However, studies over the North China Plain (NCP) are very limited (Han et al., 2008; An et al., 2013; Yan, 2013) and none of them included sensitivity studies of the chemical or physical configurations which are important to the model predictions (Misenis and Zhang, 2010; Zhang et al., 2012b). Therefore, in this study, WRF/Chem versions 3.5 and 3.5.1 that are released in April and September, 2013, respectively, are applied over East Asia and northern China at 36- and 12-km grid resolutions, respectively,

Table 1

Model configurations used in WRF/Chem simulations.

Physical and chemical processes	Baseline simulations	Sensitivity simulations
a. Physical and chemical options used in the baseline and sensitivity simulations.		
Simulation period	January 1–31, 2013	The same as baseline
Domain	East Asia (36-km), northern China (12-km)	The same as baseline
Horizontal resolution	36-km and 12-km	The same as baseline
Vertical resolution	23 layers from 1000 to 100 mb	The same as baseline
Anthropogenic emissions	MEIC [http://www.meicmodel.org/]	The same as baseline but with 30% reduction in SO ₂ , NO _x , NH ₃ , and VOCs emissions individually and collectively.
Biogenic emissions	MEGAN 2 [Guenther et al., 2006]	The same as baseline
Dust emissions	GOCART dust emissions [Ginoux et al., 2001]	The same as baseline
Sea-salt emissions	Gong (2003).	The same as baseline
Meteorological ICs and BCs	The National Centers for Environmental Prediction Final Analysis (NCEP-FNL) reanalysis data	The same as baseline
Chemical IC and BC	Default for 36-km; nested down from the parent domain for 12-km	The same as baseline
Gas-phase chemistry	SAPRC-99 [Carter, 2000]	The same as baseline
Photolysis	Madronich F-TUV [Madronich and Flocke, 1998]	The same as baseline
Aerosol module	4-bin MOSAIC aerosol with volatility basis set (VBS) [Zaveri et al., 2008; Shrivastava et al., 2011]	The same as baseline
Urban surface	Urban canopy model [Kusaka and Kimura, 2004; Ikeda and Kusaka, 2010]	The same as baseline
Shortwave radiation	RRTMG [Iacono et al., 2008]	Goddard [Chou et al., 1998]
Longwave radiation	RRTMG [Iacono et al., 2008]	RRTM [Mlawer et al., 1997]
Land surface	NOAH Land Surface Model [Chen and Dudhia, 2001; Ek et al., 2003]	Pleim-Xiu [Pleim and Xiu, 1995; Xiu and Pleim, 2001]
Surface layer	Monin-Obukhov [Monin and Obukhov, 1954; Janjic, 2001]	Pleim-Xiu [Pleim, 2006]
PBL	Yonsei University Scheme (YSU) [Hong et al., 2006]	ACM2 scheme [Pleim et al., 2007]
Cumulus	Grell 3D ensemble [Grell and Devenyi, 2002]	Grell-Devenyi ensemble [Grell and Devenyi, 2002]; Kain-Fritsch [Kain, 2004]
Microphysics	Morrison double-moment [Morrison et al., 2009]	Purdue Lin [Lin et al., 1983; Chen and Sun, 2002]; WDM6 [Lim and Hong, 2010]

Simulation index	Configuration	Notes
b. Model configurations and simulation indices in the baseline and sensitivity simulations.		
BASE	Baseline, see Table 1a	
RAD	Goddard shortwave and RRTM longwave schemes	Others are same as BASE
MP	Purdue Lin microphysics scheme	Others are same as BASE
CU_GD	Grell-Devenyi ensemble cumulus scheme	Others are same as BASE
CU_KF	Kain-Fritsch cumulus scheme	Others are same as BASE
RAD_MP_KF		

Table 1 (continued)

Simulation index	Configuration	Notes
	RAD; MP; Kain-Fritsch cumulus scheme	Others are same as BASE
RAD_MP_KF_Q (BASE_EMIS for emission sensitivity simulations)	RAD_MP_KF; nudging coefficient for Q changed from 3×10^{-4} to 1×10^{-5}	Others are same as BASE
RAD_MP_KF_TRI	RAD_MP_KF; kfeta_trigger = 2 for KF cumulus physics scheme	Others are same as BASE
RAD_WDM6_KF	RAD; WDM6 microphysics scheme; Kain-Fritsch cumulus scheme	Others are same as BASE
PX_RAD_MP_KF_351	Pleim-Xiu land surface and surface layer scheme; ACM2 PBL scheme; RAD_MP_KF; using WRF/Chem 3.5.1	Others are same as BASE
PX_RAD_MP_KF_351	Pleim-Xiu land surface and surface layer scheme; ACM2 PBL scheme; RAD_MP_KF; Nudging coefficient for Q changed from 3×10^{-4} to 1×10^{-5} ; using WRF/Chem 3.5.1	Others are same as BASE
SO ₂ _30	SO ₂ emissions are reduced by 30%	Same as BASE_EMIS
NO _x _30	NO _x emissions are reduced by 30%	Same as BASE_EMIS
NH ₃ _30	NH ₃ emissions are reduced by 30%	Same as BASE_EMIS
VOCs_30	VOCs emissions are reduced by 30%	Same as BASE_EMIS
SO ₂ _NO _x _NH ₃ _30	Emissions of SO ₂ , NO _x , and NH ₃ are reduced by 30% simultaneously	Same as BASE_EMIS
SO ₂ _NO _x _NH ₃ _VOCs_30	Emissions of SO ₂ , NO _x , NH ₃ , and VOCs are reduced by 30% simultaneously	Same as BASE_EMIS

for the extremely polluted period of January 2013, and a series of sensitivity simulations are conducted to evaluate the model performances using different physical schemes and explore relevant emission control implications. The objectives of this study are to (1) examine the sensitivities of the model predictions for both meteorology and chemical species to various physical schemes available in WRF/Chem; (2) identify an optimal set of configurations that has the best performance on both meteorology and air quality over northern China; (3) quantify the PM_{2.5} sensitivities to the reductions of emissions of major pollutants, to support the policy-making in air pollution control over this area.

The paper is organized as follows: Section 2 describes the model configurations for all simulations, and evaluation database and protocols. Section 3 presents the results from a comparative evaluation on air quality, the best set of configurations and its performance (the meteorology evaluations are in the [supplementary material](#)). Section 4 examines the sensitivities of particulate matter (PM) predictions to precursor emission reductions and implications to emission control strategies. Section 5 summarizes the major findings and limitations of this work.

2. Model description and evaluation methodology

2.1. Model configurations and simulation design

In this study, WRF/Chem simulations are performed for the period of January 2013, because the regional haze events during this period represent the most severe episode with the highest PM_{2.5} concentrations in China since 2001. A spin-up period of seven days (December 25–31, 2012) is used to minimize the influence of the initial conditions. The model inputs and configurations used in this study are shown in [Table 1a](#). As shown in [Table 1b](#), a total of 11 sensitivity simulations are conducted using various combinations

of physical schemes for East Asia with a grid resolution of 36×36 km (Domain 1, see [Fig. 1](#)). One set of configurations with the best model performance is chosen to perform nested simulations using one-way nesting over northern China that encompasses Beijing, Tianjin, and four provinces including Hebei, Henan, Shandong, and Shanxi at a 12×12 km grid resolution (Domain 2). Six sensitivity simulations in which the emissions of sulfur dioxide (SO₂), nitrogen oxide (NO_x), ammonia (NH₃), and volatile organic compounds (VOCs) are reduced by 30% individually and collectively, are then conducted over Domain 1 to examine the PM_{2.5} sensitivities to precursor emissions. The vertical resolutions in all simulations are 23 layers from the surface to the tropopause. The corresponding sigma levels are 1.000, 0.995, 0.988, 0.980, 0.970, 0.956, 0.938, 0.916, 0.893, 0.868, 0.839, 0.808, 0.777, 0.744, 0.702, 0.648, 0.582, 0.500, 0.400, 0.300, 0.200, 0.120, 0.052, and 0.000.

The accuracy of emissions is key to the reliability of the model predictions. In this study, the Multi-resolution Emission Inventory for China (MEIC) ([He, 2012; Li et al., 2014](#)) for the base year 2010 is used, following the study of L. T. [Wang et al. \(2014b\)](#). The MEIC inventory, developed by Tsinghua University, calculates all the anthropogenic emissions of eight species, including SO₂, NO_x, carbon monoxide (CO), non-methane volatile organic compounds (NMVOCs), NH₃, carbon dioxide (CO₂), PM₁₀, and PM_{2.5} in China for the years 1990–2010. Note the MEIC inventory not only contains the emission data for the above eight species, but also for the speciated chemical species of VOCs and PM for SAPRC, CB05 and RADM mechanisms ([Li et al., 2014](#)). The SAPRC99-speciated VOCs inventories are used in this study. L. T. [Wang et al. \(2014b\)](#) demonstrated that the MEIC inventory provides reasonable estimations of the total emissions from cities, but may be subject to uncertainties in the spatial allocations of those emissions into fine grid resolutions. Another uncertainty exists in the difference between the emission base year (2010) and simulation period (January 2013). The total anthropogenic emissions may have been underestimated due to the economic increase during 2010–2013 (The national GDP increased 9.3% and 7.8% in 2011 and 2012, respectively ([NBS, 2013](#))). The Model of Emissions of Gases and Aerosols from Nature (MEGAN) version 2 ([Guenther et al., 2006](#)) is used for online calculation of the biogenic emissions. Dust emissions are estimated online using the Goddard Chemistry Aerosol Radiation and Transport (GOCART) model ([Ginoux et al., 2001](#)). The sea-salt emissions are calculated using the method by [Gong \(2003\)](#).

The meteorological initial (IC) and boundary conditions (BC) are based on the National Center for Environmental Prediction (NCEP) Final Analysis (FNL) reanalysis datasets. Analysis nudging is applied for wind in and above PBL, and for temperature and water vapor mixing ratio (Q) above PBL, using the NCEP surface and upper air observation dataset (<http://dss.ucar.edu/datasets/ds351.0/>; <http://dss.ucar.edu/datasets/ds461.0/>). The default chemical profiles in WRF/Chem are used as the chemical IC and BC for the domain 1, and those for the domain 2 are nested down from the output of domain 1.

The 1999 version of the Statewide Air Pollution Research Center (SAPRC-99) mechanism ([Carter, 1990, 2000](#)) is chosen as the gas-phase chemical mechanism in this work, which is demonstrated by [Lin et al. \(2009\)](#) of better performance than the Carbon Bond 4 (CB4) over East Asia and gives satisfactory results over northern China for the haze episode simulation described in L. T. [Wang et al. \(2014b\)](#). The aerosol module is the Model for Simulating Aerosol Interactions and Chemistry (MOSAIC) that uses 4 volatility bins with the Volatility Basis Set (VBS) for organic aerosol evolution ([Zaveri et al., 2008; Shrivastava et al., 2011](#)). The Madronich Fast Troposphere Ultraviolet Visible (F-TUV) photolysis scheme is applied for photolytic rate calculation. The urban canopy model ([Kusaka and Kimura, 2004; Ikeda and Kusaka, 2010](#)) is used for

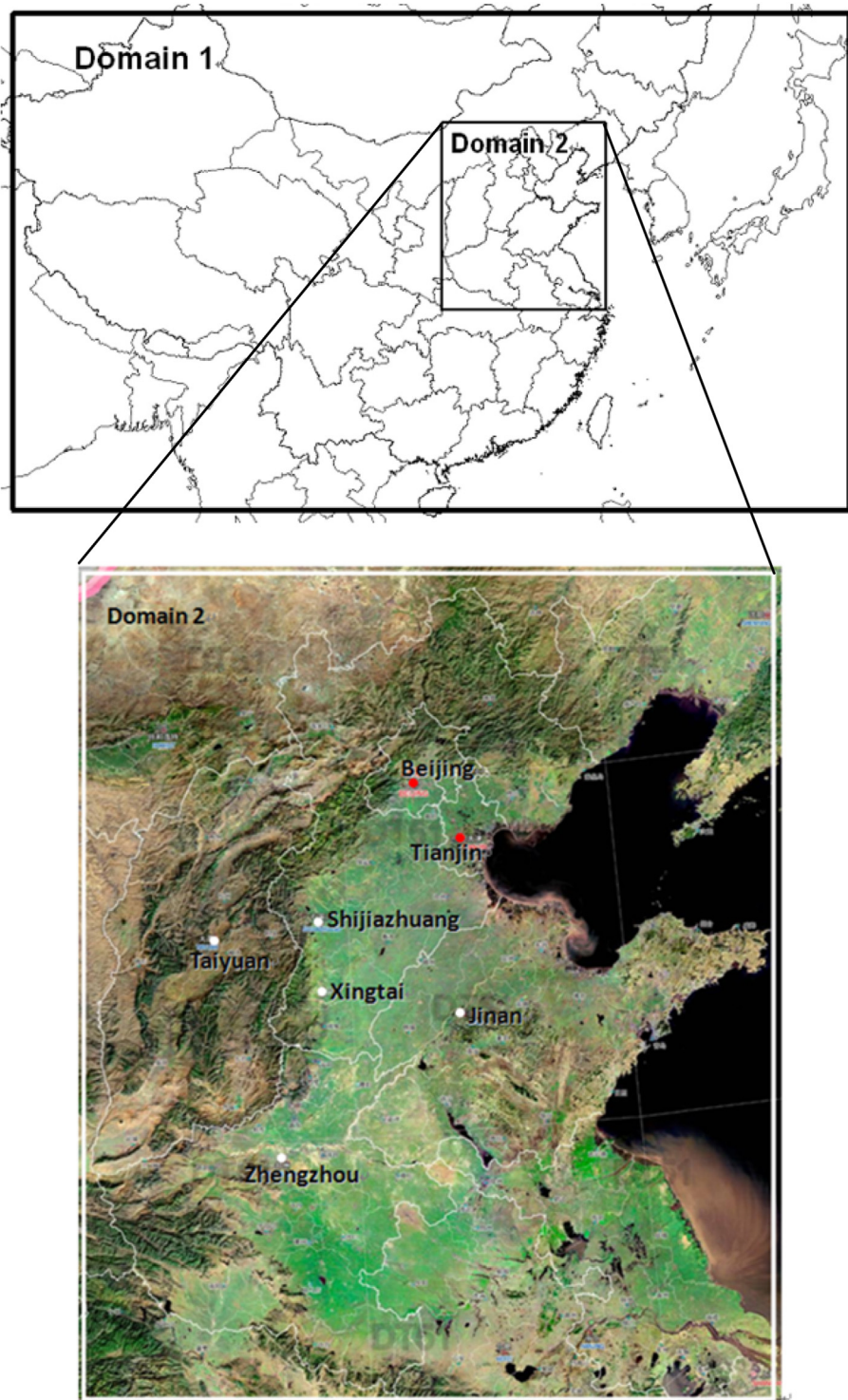


Fig. 1. WRF/Chem modeling domains at a horizontal grid resolution of 36-km over East Asia (Domain 1 with 164×97 cells) and 12-km over an area in northern China (Domain 2 with 90×108 cells).

urban surface scheme.

The baseline configurations include the RRTMG shortwave and longwave radiation schemes (Iacono et al., 2008), the Noah Land Surface Model (Chen and Dudhia, 2001; Ek et al., 2003), the Monin-Obukhov surface layer model (Monin and Obukhov, 1954; Janjic, 2001), the Yonsei University (YSU) Planetary Boundary Layer (PBL) scheme (Hong et al., 2006), the Grell 3D ensemble cumulus

parameterization (Grell and Devenyi, 2002), and the Morrison double-moment microphysics scheme (Morrison et al., 2009). The RRTMG radiation schemes, the Grell 3D ensemble cumulus parameterization, and the Morrison double-moment microphysics scheme were recently implemented in WRF/Chem to provide advanced treatments of relevant processes. The rest of physics options have been applied extensively in past studies (e.g., Grell

et al., 2005; Zhang et al., 2010a, 2012a,b; 2013). The combination of the above physics options is therefore selected as the starting point to systematically test various physics schemes and identify an optimal set of physics schemes to support WRF/Chem modeling. The sensitivity simulations are designed to use the same set of aforementioned configurations but each with an alternative physical option or a combination of several alternative options including shortwave and longwave radiation schemes, land surface and surface layer models, a PBL scheme, a cumulus parameterization, and a microphysics scheme. As shown in Table 1b, a total 10 sensitivity simulations for physical schemes and 6 simulations for emission sensitivities are performed in this study. First, the shortwave and longwave radiation schemes, microphysics scheme, and cumulus parameterization are changed one at one time to assess the changes in model performance. The schemes with better performance are then combined in several simulations to identify the best set of configurations. The nudging coefficient for Q, and the kfteta_trigger option (NCAR, 2013) in Kain-Fritsch cumulus scheme (Kain, 2004) are changed as well to improve the model predictions for precipitation. The Pleim-Xiu land surface (Pleim and Xiu, 1995; Xiu and Pleim, 2001) and surface layer (Pleim, 2006) schemes are only applied in WRF/Chem version 3.5.1 because those schemes are not fully linked in the version 3.5 and result in unrealistically high concentrations for all pollutants, e.g., the monthly average concentrations of CO over whole the BTH area are predicted as high as above 16 ppm whereas the observed CO concentrations are in the range of 0.4–5.0 ppm. The set of configurations are considered as the best when it meets the model evaluation criterias and gives the best performance statistics among all the simulations, in both meteorology and chemical predictions. The set of configurations with the best performance is then used in the emission sensitivity simulations.

In the sensitivity study, the emissions of SO₂, NO_x, NH₃, and VOC are reduced by 30%, individually and collectively, i.e., SO₂/NO_x/NH₃ and SO₂/NO_x/NH₃/VOC, to quantify the responses of the PM_{2.5} concentrations to provide scientific information in support of future emission control policy-making. 30% reduction in emissions is chosen for several reasons. First, the Action Plan for Air Pollution Prevention and Control released by the State Council on September 10, 2013 calls for a reduction of the PM_{2.5} concentrations over Beijing-Tianjin-Hebei area by 25% in 2017. In the Action Plan for Air Pollution Prevention and Control in Hebei Province published by Hebei Province following the National Action Plan, the attainment goal of PM_{2.5} concentrations in Hebei cities is set to be a reduction of 25–33% in 2017. Given those attainment goals at both national and province levels, the use of 30% emission reductions in the sensitivity represents the first attempt before a larger reduction can be justified to reach the attainment goals in a short-term, i.e., 3–5 years.

2.2. Evaluation database and protocols

The observational data used for model evaluation in this study are same to those used in L. T. Wang et al. (2014b) but for the period of January 1–31, 2013 (see Table 1, Wang et al., 2014a,b,c). The meteorological data used in this study are obtained from the National Climate Data Center (NCDC) integrated surface database. The evaluations are performed for the five major parameters: temperature at 2-m (T2), water vapor mixing ratio at 2-m (Q2), wind speed at 10-m (WS10), wind direction at 10-m (WD10), and daily precipitation. Data at every 1- or 3-h (most at 3-h) at a total of 371 sites within our domains are used in the evaluation.

As in the study of L. T. Wang et al. (2014b), two datasets of chemical concentrations are used. The first one is the real-time database from the China National Environmental Monitoring

Center (CNEMC), which began to be released since January 2013 and includes the real-time hourly concentrations of SO₂, NO₂, CO, ozone (O₃), PM_{2.5}, and PM₁₀ at 496 national monitoring stations in 74 major cities in China. The 74 cities include all the capital cities of each province, municipalities, and all the cities within the Beijing-Tianjin-Hebei area (BTH), the Yangtze River Delta (YRD), and the Pearl River Delta (PRD) (<http://113.108.142.147:20035/emcpublish/>). As mentioned in L. T. Wang et al. (2014b), CNEMC provides a much better database for model evaluation than the previous Air Pollution Index (API) database which only provides a daily index for the key pollutant on urban average for each city (Streets et al., 2007; Wang et al., 2008; Fu et al., 2009). However the main difficulty in using CNEMC is the inaccessibility of the historic data of more than 24-hr ago. This is the reason that in our study the observations for the period of January 1–13 are unavailable for the model evaluation. The second data source is the observations at a site located in the Hebei University of Engineering (refer to as HEBEU) measured by the lead author's group since July 2012 (Wei et al., 2014). More detailed descriptions of the characteristics of the site and measurement method can be found in Wei et al. (2014). The observed hourly PM_{2.5}, PM₁₀, SO₂, NO₂, and CO concentrations at this site are used in the model evaluation for the whole month of January 2013.

The meteorological evaluation is performed in terms of domainwide overall statistics. The statistical measures calculated include the Mean Bias (MB), the Root Mean Square Error (RMSE), the Normalized Mean Bias (NMB), and the Normalized Mean Error (NME), which are defined in Zhang et al. (2006). The criteria proposed by Emery et al. (2001) and Tesche et al. (2001) are used to judge meteorological performance. According to Emery et al. (2001) and Tesche et al. (2001), a satisfactory model performance should have $MB \leq \pm 0.5$ K for T2, $MB \leq \pm 1$ g kg⁻¹ for Q2, $MB \leq \pm 0.5$ m s⁻¹ for WS10, and $MB \leq \pm 10^\circ$ for WD10. The chemical evaluation is performed in terms of the overall statistics, and spatial distributions by comparing the simulated and observed concentration distributions and corresponding NMBs. In addition to NMB and NME, the Mean Fractional Bias (MFB) and the Mean Fractional Error (MFE) are analyzed, following the guidance by U. S. Environmental Protection Agency (U.S. EPA, 2007). They are also defined in Zhang et al. (2006). Boylan and Russell (2006) suggested that a model performance goal of $MFB \leq \pm 30\%$ and $MFE \leq 50\%$ and the model performance criteria of $MFB \leq \pm 60\%$ and $MFE \leq 75\%$ for PM modeling, which are used as criteria for model performance for PM and gaseous species. In addition, time series of meteorological and chemical variables at several representative sites in both domains are analyzed to assess the model performance in reproducing the temporal variations of meteorology and air quality. The evaluation of meteorology is presented in the supplementary material, and those for chemical species are in the Section 3 below.

3. Comparative evaluation of model performance

3.1. Evaluation over East Asia

As shown in Tables S1 and S2, the simulations of PX_RAD_MP_KF_Q_351 and RAD_MP_KF_Q give the best meteorological predictions among all the 11 simulations. Table 2 summarizes the domainwide statistics for chemical species, i.e., PM_{2.5}, PM₁₀, SO₂, NO₂, and CO over Domain 1 at the 36-km grid resolution. In general, the model overpredicts the concentrations of those pollutants, i.e., the concentrations of PM_{2.5} and PM₁₀ are overpredicted by the 11 simulations by 28–48% and 0–8%, respectively, and those of SO₂, NO₂, and CO are overpredicted by 33–91%, 9–27%, and 1–12%, respectively. One of the major reasons is the lack of wet scavenging scheme for the SAPRC-99 and MOSAIC-VBS option in

Table 2
Domainwide statistics of chemical predictions at a 36-km grid resolution over Domain 1.

Concentrations	Simulation name	n	Obs.	Sim.	MB	NMB (%)	NME (%)	MFB (%)	MFE (%)
PM _{2.5} (μg m ⁻³)	BASE			201.5	64.2	47	77	28	60
	RAD			195.2	57.9	42	74	26	59
	MP			186.6	49.4	36	69	22	57
	CU_GD			201.0	63.8	46	77	28	60
	CU_KF			203.0	65.8	48	78	29	60
	RAD_MP_KF	61,071	137.2	182.5	45.3	33	67	21	56
	RAD_MP_KF_Q			179.4	42.2	31	66	20	56
	RAD_MP_KF_TRI			183.4	46.1	34	68	21	57
	RAD_WDM6_KF			194.6	57.3	42	72	27	58
	PX_RAD_MP_KF_351			177.9	40.7	30	67	18	57
	PX_RAD_MP_KF_Q_351			175.1	37.8	28	66	16	57
PM ₁₀ (μg m ⁻³)	BASE			208.8	13.8	7	54	1	52
	RAD			202.5	7.5	4	52	1	52
	MP			194.8	0.2	0	51	5	52
	CU_GD			208.4	13.3	7	54	1	52
	CU_KF			210.5	15.5	8	54	2	52
	RAD_MP_KF	55,763	195.0	190.5	4.6	2	50	5	51
	RAD_MP_KF_Q			187.1	7.9	4	49	7	51
	RAD_MP_KF_TRI			191.5	3.6	2	50	5	51
	RAD_WDM6_KF			195.4	0.3	0	52	6	53
	PX_RAD_MP_KF_351			181.6	13.4	7	52	11	54
	PX_RAD_MP_KF_Q_351			178.6	16.5	8	52	13	54
SO ₂ (μg m ⁻³)	BASE			129.4	54.5	73	123	28	82
	RAD			124.2	49.4	66	119	25	82
	MP			107.9	33.1	44	106	8	82
	CU_GD			129.2	54.4	73	123	28	82
	CU_KF			129.9	55.1	74	123	28	82
	RAD_MP_KF	61,208	74.8	103.9	29.1	39	105	5	83
	RAD_MP_KF_Q			99.4	24.6	33	101	2	82
	RAD_MP_KF_TRI			104.3	29.5	39	105	5	83
	RAD_WDM6_KF			120.2	45.4	61	115	22	81
	PX_RAD_MP_KF_351			143.1	68.3	91	147	21	88
	PX_RAD_MP_KF_Q_351			139.8	65.0	87	144	19	88
NO ₂ (μg m ⁻³)	BASE			80.2	16.7	26	67	3	66
	RAD			77.3	13.8	22	64	0.3	65
	MP			71.9	8.4	13	59	4.8	63
	CU_GD			80.2	16.7	26	67	4	66
	CU_KF			80.6	17.1	27	67	4	66
	RAD_MP_KF	61,076	63.5	70.2	6.7	11	57	6.3	63
	RAD_MP_KF_Q			69.3	5.8	9	56	6.5	62
	RAD_MP_KF_TRI			70.3	6.8	11	57	6.3	63
	RAD_WDM6_KF			77.0	13.5	21	64	0.2	65
	PX_RAD_MP_KF_351			72.2	8.7	14	57	1.2	61
	PX_RAD_MP_KF_Q_351			70.9	7.4	12	56	1.9	60
CO (mg m ⁻³)	BASE			2.5	0.3	12	64	-1.8	61
	RAD			2.4	0.2	7	62	-4.8	60
	MP			2.4	0.1	5	61	-6.1	60
	CU_GD			2.5	0.3	11	64	-1.7	61
	CU_KF			2.6	0.3	12	64	-1.0	61
	RAD_MP_KF	61,529	2.3	2.3	0.0	2	59	-7.7	60
	RAD_MP_KF_Q			2.3	0.0	1	59	-8.4	59
	RAD_MP_KF_TRI			2.3	0.1	2	60	-7.6	60
	RAD_WDM6_KF			2.4	0.1	5	61	-5.3	60
	PX_RAD_MP_KF_351			2.5	0.2	11	66	-3.8	62
	PX_RAD_MP_KF_Q_351			2.5	0.2	10	66	-4.1	62

WRF/Chem 3.5 and 3.5.1 (Peckham et al., 2013). Saide et al. (2012) evaluated the influence of wet deposition to atmospheric concentrations of gaseous and aerosol species by simulations with/without wet scavenging process using WRF/Chem. They found that significant differences existed in SO₂ and aerosol concentrations when the wet deposition process was turned off. Therefore, the uncertainties introduced by the lack of wet scavenging should be considered in model evaluation, as well as distinguishing them from the uncertainties from the emission inventory. The uncertainties of the MEIC emission inventory are estimated to be smaller or same to the INTEX-B emission inventory, which are ±12% for SO₂, ±31% for NO_x, ±68% for NMVOCs, ±70% for CO, ±132% for PM₁₀, ±130% for PM_{2.5} for China (Q. Zhang et al., 2009a private communication, Qiang Zhang, Tsinghua University, China,

September, 2014). Although large uncertainties may exist in the primary PM emission inventory, the secondary inorganic and organic aerosols, generated from the gaseous precursors which have much smaller uncertainties, are believed to be the driving factors during this severe polluted month (Huang et al., 2014; Zheng et al., 2014). The modeling results over the same domains for the same period using the exactly same inventory and same chemical mechanism but with the MM5-CMAQ system that includes wet scavenging process (L. T. Wang et al., 2014b) showed that PM_{2.5} are slightly underpredicted over Domain 1 (with an NMB of -14.6%) and over-estimated over Domain 2 (with an NMB of 19.1%). These results may imply that the range of the uncertainties introduced by the MEIC inventory, which cannot explain WRF/Chem performance (i.e., the RAD_MP_KP_Q simulation) with the

NMB of 31% for Domain 1 and 45% for Domain 2 in this work, the lack of wet scavenging is most likely responsible for the over-predictions in PM_{2.5} concentrations.

As shown in Table 2, the averaged observed PM_{2.5} concentration over Domain 1 is 137.2 $\mu\text{g m}^{-3}$, and that of the baseline prediction is 201.5 $\mu\text{g m}^{-3}$, with 47% of overprediction. Changing in the radiation, microphysics and cumulus schemes individually, i.e., RAD, MP, and CU_GD, will result in a slightly better performance (186.6–201.0 $\mu\text{g m}^{-3}$). The combined configurations used in RAD_MP_KF and the reduction in nudging coefficient of Q used in RAD_MP_KF_Q further reduce the overprediction (182.5 and 179.4 $\mu\text{g m}^{-3}$, respectively) and the changing in nudging coefficient of Q (RAD_MP_KF_Q) results in the PM_{2.5} concentration of 179.4 $\mu\text{g m}^{-3}$. Although there is a large discrepancy on the precipitation predictions between the two simulations (0.7 vs. 1.3), the concentrations of PM_{2.5} are not changed significantly due to the lack of wet scavenging for these options in this version of WRF/Chem. Our study indirectly attests the importance of wet scavenging process to pollutants concentrations, which should be one of the foci and priorities for model improvement for the SAPRC99-MOSAIC/VBS option. While NMBs and NMEs are 28–47% and 66–78%, respectively, MFBs are 16–29% and MFEs are 57–60% for PM_{2.5} predictions from all simulations. The performance of PM_{2.5} predictions by all those simulations is considered to be satisfactory based on the performance criteria of an MFB within $\pm 60\%$ and an MFE within 75% proposed by Boylan and Russell (2006). Among the 11 simulations, the simulations with the best performance for PM_{2.5} are PX_RAD_MP_KF_Q_351, PX_RAD_MP_KF_351, and RAD_MP_KF_Q, which have the lowest NMBs, NMEs, MFBs, and MFEs. Compared to PM_{2.5} performance, the predictions for PM₁₀ show much improved performance statistics with small differences among the 11 simulations. The smaller biases (NMBs of 0–8%) in PM₁₀ predictions indicate bias compensation, i.e., the relatively large overpredictions in the PM_{2.5} concentrations are compensated by large underpredictions in those of PM_{2.5-10} (e.g., mineral dust).

As for SO₂, the observation is 74.8 $\mu\text{g m}^{-3}$ and baseline prediction is 129.4 $\mu\text{g m}^{-3}$, with an NMB of 73%. Changes in radiation and cumulus parameterizations, i.e., RAD, CU_GD, and CU_KF, do not evidently improve the results (124.2–129.9 $\mu\text{g m}^{-3}$), but using a different microphysics scheme from BASE in MP (i.e., the Purdue Lin microphysics scheme), greatly reduces the overprediction (107.9 $\mu\text{g m}^{-3}$, with an NMB of 44%), although the overprediction remains. The simulations of RAD_MP_KF, RAD_MP_KF_Q, and RAD_MP_KF_TRI give slightly better results (99.4–104.3 $\mu\text{g m}^{-3}$). The simulations with the WDM6 microphysics scheme (RAD_WDM6_KF) and the Pleim-Xiu land surface and surface layer schemes (PX_RAD_MP_KF_351 and PX_RAD_MP_KF_Q_351) do not give better predictions for SO₂, with NMBs of 61–91%. The simulation RAD_MP_KF_Q gives the best performance for SO₂ predictions. The MFBs and MFEs of all the simulations are in the range of 2–28% and 81–88%, respectively, which are within the criteria of MFB $\leq \pm 60\%$ and slightly over the criteria of MFE $\leq 75\%$ proposed by Boylan and Russell (2006). The overpredictions of NO₂ are not as significant as those for SO₂ with NMBs of 9–27%. Similar to SO₂, NO₂ predictions are more sensitive to the choice of microphysics schemes. The simulation with the Purdue Lin scheme (MP) performs better than the Morrison double moment used in BASE and the WDM6 used in RAD_WDM6_KF. In general, the RAD_MP_KF_Q shows the best performance in terms of NO₂ predictions with an NMB of only 9%. The predictions of CO agree well with observations, with NMBs of 1–12% of all the simulations. The observed and simulated concentrations of CO by the BASE simulation are 2.3 and 2.5 mg m^{-3} , respectively, with an NMB of 12%. Changing in radiation and microphysics, i.e., RAD and MP, will improve the results (NMBs of 5–7%), but the alternation in cumulus parameterizations

(CU_GD, CU_KF) will not result in a significant improvement (NMBs of 11–12%). The combined simulations of RAD_MP_KF, RAD_MP_KF_Q, and RAD_MP_KF_TRI further reduce the NMBs to 1–2%. The RAD_MP_KF_Q shows the best performance. The MFBs and MFEs of NO₂ and CO predictions are all within the criteria of MFB $\leq \pm 60\%$ and MFE $\leq 75\%$ (Boylan and Russell, 2006).

Among the 11 simulations, the optimal configuration set with the best overall performance in terms of both meteorological and chemical predictions is RAD_MP_KF_Q. Therefore, this configuration is chosen for nested simulations at 12-km and emission sensitivity simulations at 36-km. Fig. 2 presents the overlay of the predicted and observed monthly average concentrations of the four major pollutants and their corresponding NMBs from RAD_MP_KF_Q. The model generally well reproduces the spatial distributions of the four pollutants, especially for PM₁₀, NO₂, and CO. The overprediction of PM_{2.5} mostly appears in the north and central China, e.g., Shanxi, Henan, southern Hebei, northern Anhui, and the cities along the Yangtze River. The SO₂ concentrations over southern Hebei are underpredicted, and the overprediction occurs in the Northeast China, Shanxi, and also the cities along the Yangtze River. The time series of the observed and simulated (RAD_MP_KF_Q) concentrations at the representative cities in Domain 1 are presented in the Section 4 of the supplementary material.

3.2. Evaluation over northern China

The meteorological evaluation for Domain 2 are in Section 2 of the supplementary material. It indicates that the RAD_MP_KF_Q configuration shows the best performance over Domain 2 and the nested simulation at a 12-km grid resolution improves the predictions for temperature and humidity, and performs similarly for other meteorological predictions. The improvements on meteorological predictions of the RAD_MP_KF_Q comparing with the BASE in terms of NMB are summarized in Table 3, for both Domain 1 and 2. In general, the model performances are improved in terms of T2 and precipitation, not changed for WD10, and slightly declined for Q2 and WS10. The most significant improvement is for precipitation, with NMBs decreased from –76% to –3% over Domain 1 (at 36-km grid resolution), and –82% to 19% (at 36-km grid resolution) and 21% (at 12-km grid resolution) over Domain 2.

The statistics over Domain 2 for chemical variables are shown in Table 4. In general, the model overpredicts the concentrations of all species over the Domain 2 at a 36-km grid resolution, with NMBs of 45–70% for PM_{2.5}, 3–23% for PM₁₀, 32–114% for SO₂, 36–61% for NO₂, and 18–74% for CO. The NMB of RAD_MP_KF_Q for PM_{2.5} is 50% at 36-km and reduces to 23% at 12-km. The MFBs and MFEs for PM_{2.5} predictions from all the 36-km simulations are 23–48% and 58–64%, respectively, which are still within the threshold for satisfactory performance proposed by the U.S. EPA (2007) and Boylan and Russell (2006). The NMBs for PM₁₀ are much smaller than for PM_{2.5}, indicating that the model underpredicts the concentrations of PM_{2.5-10}. The NMBs of RAD_MP_KF_Q for PM₁₀ are 9% at 36-km, and 4% at 12-km. As for SO₂, RAD_MP_KF_Q performs the best among all the simulations at 36-km, with an NMB of 32%, an MFB of 22% (within the criteria of MFB $\leq \pm 60\%$), and an MFE of 76% (slightly over the criteria of MFE $\leq 75\%$), but the NMB at 12-km dramatically increases to 113.4% (with an MFB of 30% and an MFE of 93%). Fig. 3 presents the overlay of the simulated and observed monthly average concentrations of PM_{2.5}, PM₁₀, SO₂, NO₂, and CO at the 36- and 12-km grid resolutions over Domain 2, and the corresponding NMBs. The model generally captures the spatial distributions of SO₂ pollution (Fig. 3a–b). The significant change of NMBs mostly occurs in Hebei area (Fig. 3c–d), where the model underpredicts the SO₂ concentrations over most of the cities in Hebei area

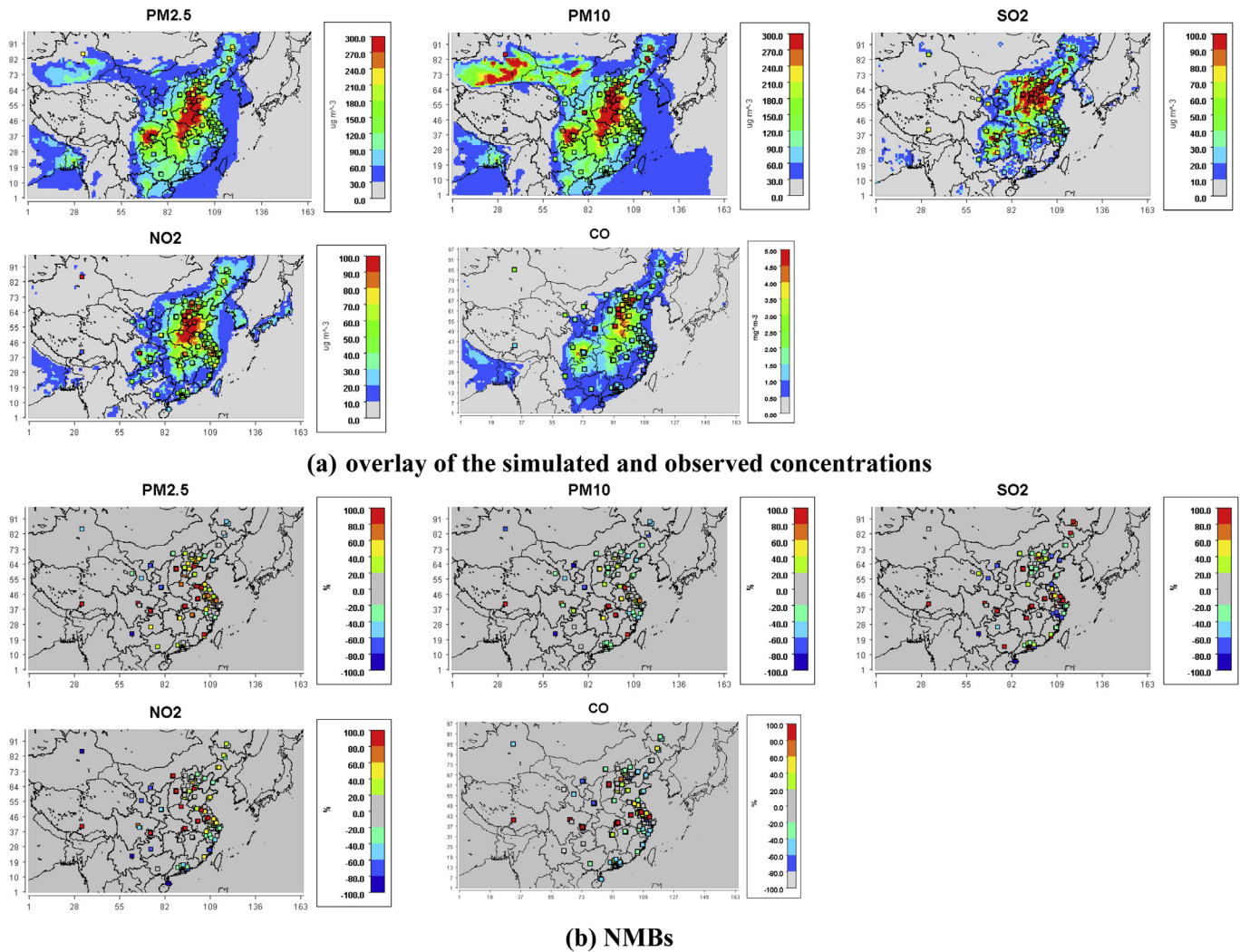


Fig. 2. Overlay of the simulated (RAD_MP_KF_Q) and observed monthly average concentrations of PM_{2.5}, PM₁₀, SO₂, NO₂, and CO (a) and their NMBs (b) over the Domain 1 at 36-km grid resolution.

Table 3

Comparison of model performance on meteorological predictions of the RAD_MP_KF_Q and the BASE simulations in terms of NMB over Domain 1 at 36-km grid resolution, and Domain 2 at 36- and 12-km grid resolutions.

Simulation Name	East Asia (Domain 1)		Northern China (Domain 2)		
	BASE	RAD_MP_KF_Q	BASE (36-km)	RAD_MP_KF_Q (36-km)	RAD_MP_KF_Q (12-km)
T2	-77	-61	-55	-46	-33
Q2	12	14	8	12	11
WS10	33	35	1	4	5
WD10	2	2	-0.2	0.1	-0.4
Precipitation	-76	-3	-82	-19	-21

at 36-km, but it shows noticeable overpredictions when nesting to 12-km. Since SO₂ is more sensitive to the local source emissions, this change implies that uncertainties exist in the spatial allocations of the emissions into a finer grid resolution. It may overestimate the SO₂ emissions in the urban grids if the population density was used as a surrogate to distribute the emissions into a finer grid resolution, as discussed in L. T. Wang et al. (2014b). The distribution of NMBs for NO₂ and CO also shows the similar characteristics between predictions at 36- and 12-km, despite to a lesser

extent comparing to those for SO₂. The NMBs, MFBs, and MFEs of NO₂ predictions from RAD_MP_KF_Q are 36%, 27%, and 55% at 36-km, and 40%, 12%, and 64% at 12-km, respectively, and those for CO are 18%, 16%, and 55% at 36-km, and 36%, 10%, and 65% for 12-km, respectively. In general, the model gives reasonable predictions and RAD_MP_KF_Q performs the best among all the 36-km simulations over the Domain 2. The nested simulation at 12-km further improves the performances for PM_{2.5} and PM₁₀ but deterioration occurs for SO₂, NO₂, and CO due partially to the uncertainties in the spatial distribution of the emissions into the fine grid resolution. The summary of model performance improvements of RAD_MP_KF_Q comparing with the BASE in terms of NMB over both Domain 1 and 2 is presented in Table 5. The time series of the observed and simulated (RAD_MP_KF_Q) concentrations at the representative cities within Domain 2 are presented in the Section 5 of the supplementary material.

4. Emission sensitivity and policy implications

Fig. 4 shows the PM_{2.5} concentrations simulated by the optimal configuration, i.e., RAD_MP_KF_Q (hereafter BASE_EMIS) and their sensitivities to the emission reductions (by 30%) of SO₂, NO_x, NH₃, and VOCs individually and collectively, i.e., emissions of SO₂, NO_x,

Table 4
Domainwide statistics of chemical predictions over Domain 2 at 36- and 12-km grid resolutions.

Concentrations	Simulation name	Resolution (km)	n	Obs.	Sim.	MB	NMB (%)	NME (%)	MFB (%)	MFE (%)
PM _{2.5} (μg m ⁻³)	BASE	36			263.8	108.5	70	89	48	64
	RAD	36			255.5	100.2	65	84	45	62
	MP	36			244.8	89.5	58	79	42	60
	CU_GD	36			262.9	107.5	69	88	48	64
	CU_KF	36			264.9	109.6	71	89	48	64
	RAD_MP_KF	36	50,433	155.3	236.6	81.3	52	75	40	59
	RAD_MP_KF_TRI	36			238.0	82.7	53	75	40	59
	RAD_WDM6_KF	36			252.4	97.1	62	82	45	61
	PX_RAD_MP_KF_351	36			227.9	72.5	47	73	35	58
	PX_RAD_MP_KF_Q_351	36			226.0	70.7	46	72	34	58
	RAD_MP_KF_Q	36			233.5	78.2	50	73	39	58
	RAD_MP_KF_Q	12			225.7	70.4	45	79	23	63
	PM ₁₀ (μg m ⁻³)	BASE	36			271.9	49.8	22	55	19
RAD		36			263.9	41.7	19	53	17	50
MP		36			254.0	31.8	14	50	14	49
CU_GD		36			270.9	48.7	22	55	19	51
CU_KF		36			272.9	50.8	23	55	20	51
RAD_MP_KF		36	43,519	222.1	245.7	23.6	11	49	11	48
RAD_MP_KF_TRI		36			247.1	25.0	11	50	12	49
RAD_WDM6_KF		36			262.1	40.0	18	52	17	49
PX_RAD_MP_KF_351		36			231.6	9.4	4	51	4	51
PX_RAD_MP_KF_Q_351		36			229.4	7.3	3	51	3	51
RAD_MP_KF_Q		36			241.9	19.7	9	48	10	48
RAD_MP_KF_Q		12			231.7	9.6	4	56	-6	56
SO ₂ (μg m ⁻³)		BASE	36			167.4	68.2	69	110	45
	RAD	36			161.5	62.3	63	106	42	81
	MP	36			145.3	46.1	46	97	30	78
	CU_GD	36			167.1	67.9	68	110	45	82
	CU_KF	36			168.1	68.9	69	110	45	82
	RAD_MP_KF	36	50,390	99.2	138.1	38.8	39	94	26	77
	RAD_MP_KF_TRI	36			138.8	39.6	40	95	26	78
	RAD_WDM6_KF	36			155.1	55.8	56	102	39	79
	PX_RAD_MP_KF_351	36			181.2	82.0	83	128	41	85
	PX_RAD_MP_KF_Q_351	36			175.3	76.1	77	124	38	84
	RAD_MP_KF_Q	36			131.2	32.0	32	89	22	76
	RAD_MP_KF_Q	12			212.6	113.4	114	165	30	93
	NO ₂ (μg m ⁻³)	BASE	36			105.6	40.0	61	78	40
RAD		36			101.6	36.0	55	73	38	60
MP		36			93.8	28.2	43	65	31	57
CU_GD		36			105.5	39.9	61	78	40	62
CU_KF		36			105.8	40.2	61	78	41	62
RAD_MP_KF		36	50,442	63.5	90.6	25.0	38	62	28	55
RAD_MP_KF_TRI		36			90.9	25.3	39	62	29	55
RAD_WDM6_KF		36			101.1	35.5	54	72	38	59
PX_RAD_MP_KF_351		36			90.9	25.3	39	63	29	55
PX_RAD_MP_KF_Q_351		36			89.3	23.7	36	61	27	55
RAD_MP_KF_Q		36			89.4	23.8	36	60	27	55
RAD_MP_KF_Q		12			91.8	26.2	40	75	12	64
CO (mg m ⁻³)		BASE	36			3.6	0.9	32	66	25
	RAD	36			3.4	0.7	26	64	22	58
	MP	36			3.4	0.7	25	62	21	57
	CU_GD	36			3.5	0.8	30	74	22	67
	CU_KF	36			3.6	0.9	32	67	26	59
	RAD_MP_KF	36	50,584	2.7	3.2	0.5	19	59	17	56
	RAD_MP_KF_TRI	36			3.2	0.5	20	59	18	56
	RAD_WDM6_KF	36			3.3	0.6	22	69	18	64
	PX_RAD_MP_KF_351	36			3.5	0.8	28	67	21	60
	PX_RAD_MP_KF_Q_351	36			3.5	0.8	29	69	21	60
	RAD_MP_KF_Q	36			3.2	0.5	18	58	16	55
	RAD_MP_KF_Q	12			3.7	1.0	36	81	10	65

NH₃, and VOCs are reduced by 30% individually (i.e., the simulations SO₂_30, NO_x_30, NH₃_30, and VOCs_30, respectively), those of SO₂, NO_x, and NH₃, are reduced simultaneously (i.e., the simulation SO₂_NO_x_NH₃_30), and those of SO₂, NO_x, NH₃, and VOCs are reduced by 30% simultaneously (i.e., the simulation SO₂_NO_x_NH₃_VOCs_30). It should be noted that lack of wet scavenging will extend the lifetime of atmospheric aerosols and soluble gaseous pollutants. The increase of the lifetime of some precursors of PM_{2.5}, e.g., SO₂, NO₂, NH₃, and VOCs, will result in differences in atmospheric chemistry and thus PM_{2.5} composition

and concentrations (Knote and Brunner, 2013; Garrett et al., 2006). And extend of PM_{2.5} lifetime will lead to the changes in radiation, cloud process, etc., in online-coupled simulations. Although it will affect the performance statistics of a single simulation, it will not lead to significant differences in predicted sensitivities, as both the baseline and sensitivity simulations do not include wet scavenging.

As shown in Fig. 4b, the largest reduction in SO₂ concentrations due to 30% reductions in SO₂ emissions occurs in the Sichuan Basin, southern Hebei, Hubei, and northern Hunan, at the level of 2–15 μg m⁻³, which is about 2.5–10% of the PM_{2.5} concentrations

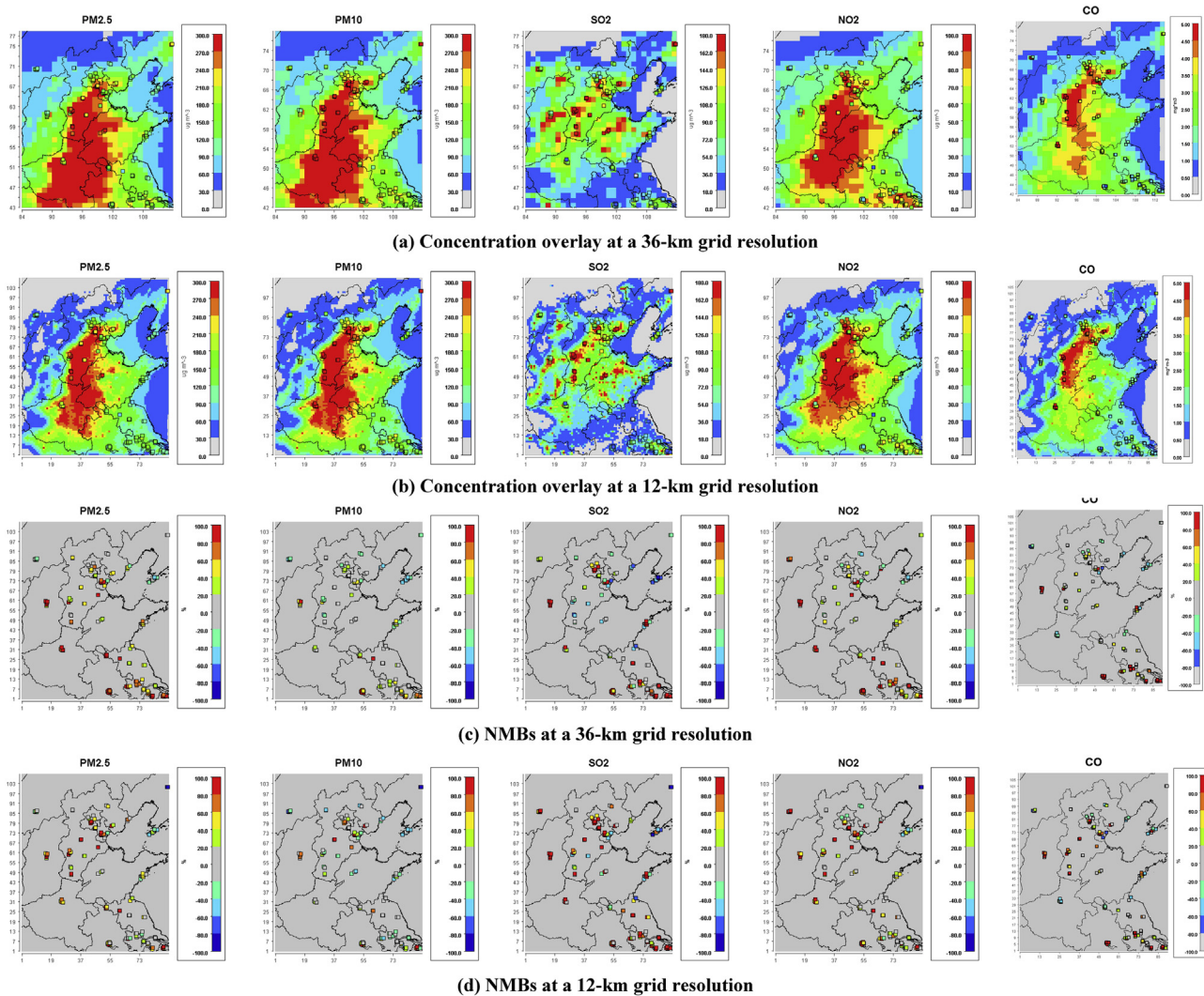


Fig. 3. Overlay of the simulated (RAD_MP_KF_Q) and observed monthly average concentrations of PM_{2.5}, PM₁₀, SO₂, NO₂, and CO, and their NMBs over the Domain 2 at 36- and 12-km grid resolutions ((a) and (b), respectively), and NMBs at 36- and 12-km grid resolutions ((c) and (d), respectively).

predicted by BASE_EMIS. These results show that 30% reduction of SO₂ emissions will not result in significant decreases in PM_{2.5} concentrations.

Emission reduction of NO_x will lead to a notable increase (instead of decrease) in PM_{2.5} concentrations over the NCP, especially southern area of Hebei, Shandong, and northern area of Henan. The increases are 2–25 $\mu\text{g m}^{-3}$, which are 2.5–8.3% of the PM_{2.5} concentrations from BASE_EMIS. This is because the NCP area is under the NH₃-rich and VOC-limited conditions which are discussed in Section 6 in the supplementary material.

It should be noted that the observational data of the indicators mentioned in the Section 6 in the supplementary material are not available over China to verify simulated model sensitivity. However, the observations of another indicator, i.e., the ratios of column mass abundance of HCHO/NO₂ (Tonnesen and Dennis, 2000a, b; Y. Zhang et al., 2009b, 2010b), can be calculated from the satellite observed column mass concentrations of HCHO and NO₂. Fig. 5 compares the simulated and observed tropospheric column mass abundance of HCHO and NO₂, and their ratios. The observed column mass abundances are derived from the Ozone Monitoring Instrument (OMI) on the Aura satellite launched by the National Aeronautics

Table 5

Comparison of model performance on air quality predictions of the RAD_MP_KF_Q and the BASE simulations in terms of NMB over Domain 1 at 36-km grid resolution, and Domain 2 at 36- and 12-km grid resolutions.

Simulation Name	East Asia (Domain 1)		Northern China (Domain 2)		
	BASE	RAD_MP_KF_Q	BASE (36-km)	RAD_MP_KF_Q (36-km)	RAD_MP_KF_Q (12-km)
PM _{2.5}	47	31	70	50	45
PM ₁₀	7	4	22	9	4
SO ₂	73	33	69	32	114
NO ₂	26	9	61	36	40
CO	12	1	32	18	36

and Space Administration. Both HCHO and NO₂ columns are level-3 monthly averaged retrieval data available to the public, which are then interpolated to the 36-km grid resolution using the bilinear interpolation of the NCAR command language (<http://www.ncl.ncar.edu>). Fig. 5 indicates that the model predictions agree quite well in terms of not only the tropospheric column of HCHO and NO₂, but also their ratios, especially over northern China. The values of HCHO/NO₂ over the NCP are around 0.5, which clearly indicates the VOC-limited regime (HCHO/NO₂ < 1). This is also consistent with the studies of Zhang et al. (2009a,b), Liu et al. (2010), and Zhao

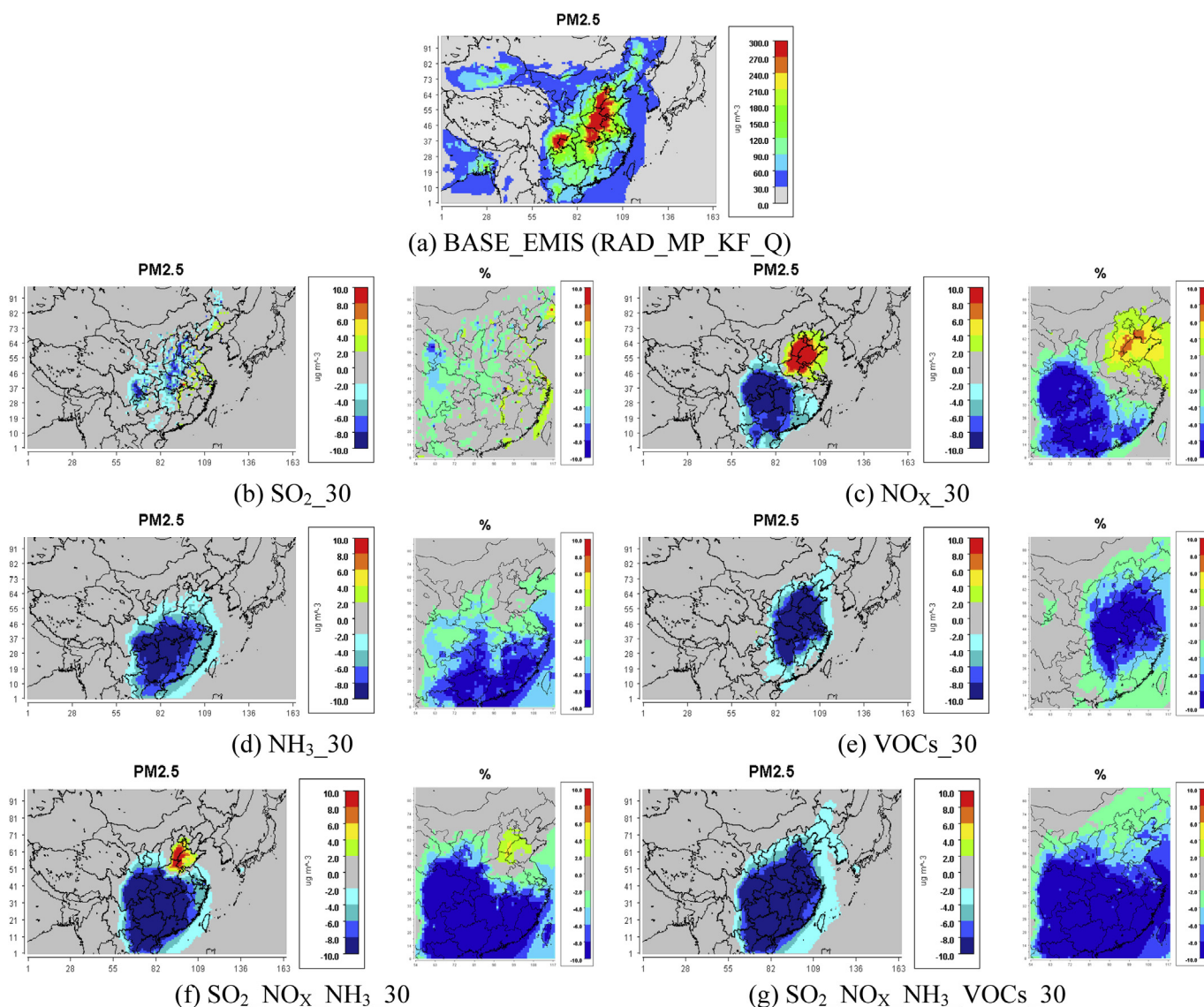


Fig. 4. $PM_{2.5}$ concentrations and the sensitivities to the emission changes of SO_2 , NO_x , NH_3 , and VOCs over the Domain 1 by RAD_MP_KF_Q simulation (emission reduction simulation – BASE_EMIS). (a) The predicted baseline $PM_{2.5}$ concentrations. Change in $PM_{2.5}$ concentrations and percentages when (b) SO_2 emissions are reduced by 30%. (c) NO_x emissions are reduced by 30%. (d) NH_3 emissions are reduced by 30%. (e) VOCs emissions are reduced by 30%. (f) SO_2 , NO_x , and NH_3 emissions are reduced by 30% simultaneously. (g) SO_2 , NO_x , NH_3 , and VOCs emissions are reduced by 30% simultaneously.

et al. (2013).

Therefore, the reduction of NO_x emissions will result in an increase in the concentrations of oxidants such as O_3 and HO_x . The elevated concentrations of those oxidants and radicals accelerate the generation of secondary organic and inorganic aerosols such as sulfate and nitrate, which compensates the effect of the decreased NO_x concentrations on the nitrate formation. The declined $PM_{2.5}$ concentrations occur over southern China such as eastern area of Sichuan, Chongqing City, Guizhou, Guangxi, and Hunan, by $5\text{--}30\ \mu\text{g m}^{-3}$ (by 5–13%) which is also consistent with the results of Zhao et al. (2013).

$PM_{2.5}$ concentrations are more sensitive to reductions in NH_3 emissions in southern China, i.e., along and in regions located in the south of the Yangtze River. A 30% reduction of NH_3 emissions results in a decrease of roughly $5\text{--}15\ \mu\text{g m}^{-3}$ in $PM_{2.5}$ concentrations, accounting for 2–8% of baseline $PM_{2.5}$ concentrations. There are not significant changes in $PM_{2.5}$ concentrations over NCP, due to the NH_3 -rich condition over this area. Reduction in VOCs emissions, as

shown in Fig. 4e, reduces $PM_{2.5}$ concentrations over eastern China, especially over NCP, Henan, Jiangsu, and Anhui, by $5\text{--}50\ \mu\text{g m}^{-3}$ (by 4–18%) which is consistent with the VOC-limited regime where the reduced VOCs concentrations result in a decrease in oxidant concentrations that leads to the decrease of sulfate and nitrate concentrations. The secondary organic aerosols are decreased, due to decreases in both oxidants concentrations and primary VOCs emissions.

The combined emission controls, e.g., reducing SO_2 , NO_x , and NH_3 emissions simultaneously by 30%, reduce the $PM_{2.5}$ concentrations over southern China by $5\text{--}40\ \mu\text{g m}^{-3}$ (2–17%, see Fig. 4f), but slightly increase those in the intersection area of Hebei, Henan, and Shandong provinces, due to the characteristics of NH_3 -rich and VOC-limited conditions in those areas. When emissions of the four primary pollutants, SO_2 , NO_x , NH_3 , and VOC are controlled simultaneously, as shown in Fig. 4g, the $PM_{2.5}$ concentrations decrease over most areas of eastern and southern China, by $5\text{--}41\ \mu\text{g m}^{-3}$, which corresponds to 2–17% of the $PM_{2.5}$ concentrations predicted

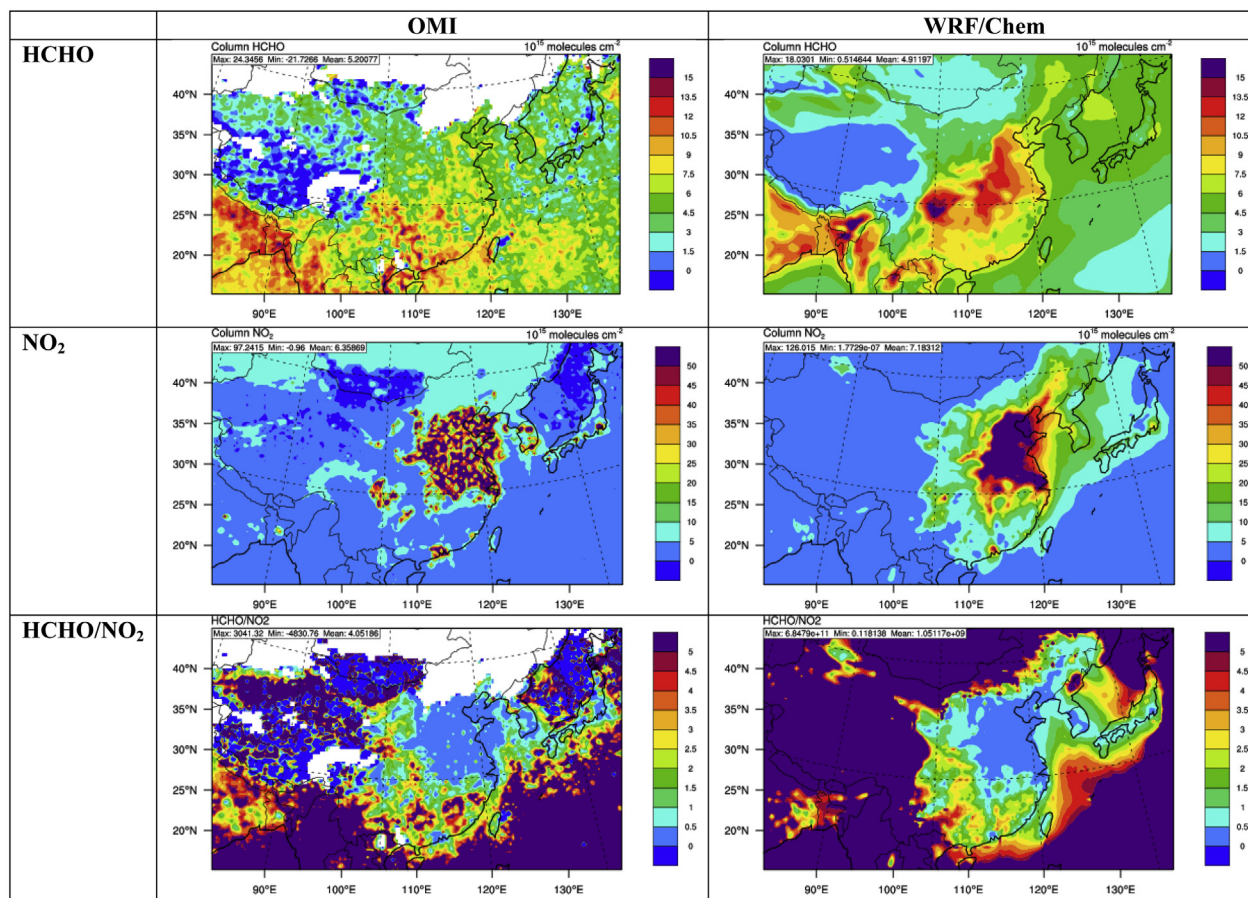


Fig. 5. Spatial distribution of the simulated (RAD_MP_KF_Q) and satellite observed monthly mean column mass abundances of HCHO, NO₂ and HCHO/NO₂ over Domain 1.

by BASE_EMIS. These results imply that NO_x emissions controls, which are considered to be one of the major tasks in the China national pollution control plan (Zhao et al., 2013), should be accompanied with the controls of other pollutants, especially VOCs, which is important to reduction of the severe PM_{2.5} pollution during the winter time over NCP, the top polluted area in China.

5. Conclusions

In this study, the online-coupled meteorology-air quality model, WRF/Chem, is applied to simulate the extremely severe haze pollution in January 2013 over East Asia and the north China at 36- and 12-km grid resolutions, respectively. A total of 11 simulations are conducted to examine the sensitivities of the model predictions to the physical schemes, i.e., shortwave and longwave radiation schemes, land surface and surface layer models, planetary boundary layer scheme, cumulus parameterization, and microphysics scheme. The results show that all simulations perform similarly for T2, Q2, WS10, and WD10, but give substantially different precipitation predictions. Using a smaller nudging coefficient of 1×10^{-5} for water vapor mixing ratio, instead of the original 3×10^{-4} , significantly reduces the negative bias of precipitation predictions. The concentrations of four major pollutants, PM_{2.5}, PM₁₀, SO₂, NO₂, and CO are overpredicted due mainly to the lack of wet scavenging for the SAPRC99-MOSAIC/VBS option in WRF/Chem versions 3.5 and 3.5.1. The optimal configuration with the best overall performance identified in this work is RAD_MP_KF_Q, that is, the simulation with the Goddard shortwave and RRTM longwave radiation schemes, the Purdue Lin microphysics scheme, the Kain-Fritsch

cumulus scheme, and a nudging coefficient of 1×10^{-5} for water vapor mixing ratio. The nested simulation at the 12-km resolution improves the performance for PM_{2.5} and PM₁₀ but deteriorates that for SO₂, NO₂, and CO, partially because of the uncertainties in the spatial allocation of the emissions into a finer grid resolution.

The results of emission sensitivity simulations show that PM_{2.5} levels in northern China are more sensitive to the emissions of NO_x, SO₂, and VOCs than those of NH₃. While a 30% reduction in the emissions of SO₂ and VOCs leads to a decrease of 2–15 $\mu\text{g m}^{-3}$ and 5–50 $\mu\text{g m}^{-3}$, respectively, in PM_{2.5} concentrations, NO_x emission reduction adversely increases the PM_{2.5} concentrations by 2–25 $\mu\text{g m}^{-3}$, due to the NH₃-rich and VOC-limited atmospheric conditions over northern China. In southern China, PM_{2.5} concentrations are more sensitive to emissions of NO_x and NH₃. A 30% reduction of NO_x emissions leads to a decrease of 5–30 $\mu\text{g m}^{-3}$ in PM_{2.5} concentrations and the reduction of NH₃ emissions results in a decrease of roughly 5–15 $\mu\text{g m}^{-3}$. Reductions of VOCs emissions reduce PM_{2.5} over eastern China by about 5–50 $\mu\text{g m}^{-3}$. While the combined emission controls of SO₂, NO_x, and NH₃ by 30% leads to a large reduction in PM_{2.5} concentrations over southern China, it increases PM_{2.5} concentrations in northern China. When the emissions of SO₂, NO_x, NH₃, and VOCs are controlled simultaneously, the PM_{2.5} concentrations decrease over most areas of eastern and southern China by roughly 5–41 $\mu\text{g m}^{-3}$ (by 2–17%). The results in this work indicate that more aggressive, combined emission control strategies are needed to mitigate the severe pollution over northern China to reach the objective of 25% PM_{2.5} concentration reduction in 2017 proposed in the Action Plan for Air Pollution Prevention and Control by the State Council in 2013.

Acknowledgments

This study was co-sponsored by the National Natural Science Foundation of China (No. 41475131, 41105105), the Natural Science Foundation of Hebei Province (No. D2011402019), the State Environmental Protection Key Laboratory of Sources and Control of Air Pollution Complex (No. SCAPC201307), the Excellent Young Scientist Foundation of Hebei Education Department (No. YQ2013031), the Program for the Outstanding Young Scholars of Hebei Province, the China Scholarship Council, and the Handan Environmental Protection Bureau at HEBEU, China, and the U.S. DOE climate modeling programs (DESC0006695) at NCSU, U.S.A. Thanks are due to Robert Gilliam, the U.S. EPA, for providing valuable suggestions to apply a lower nudging coefficient to improve precipitation predictions.

This study used computer resources of the National Energy Research Scientific Computing Center (HOPPER), which is supported by the Office of Science of the U.S. Department of Energy under Contract No. DE-AC02-05CH11231, and the Extreme Science and Engineering Discovery Environment (XSEDE) (STAMPEDE), which is supported by National Science Foundation grant number OCI-1053575.

Appendix A. Supplementary data

Supplementary data related to this article can be found at <http://dx.doi.org/10.1016/j.atmosenv.2014.12.052>.

References

- An, J.L., Li, Y., Chen, Y., Li, J., Qu, Y., Tang, Y.J., 2013. Enhancements of major aerosol components due to additional HONO sources in the North China Plain and implications for visibility and haze. *Adv. Atmos. Sci.* 30 (1), 57–66.
- Boylan, J.W., Russell, A.G., 2006. PM and light extinction model performance metrics, goals, and criteria for three-dimensional air quality models. *Atmos. Environ.* 40, 4946–4959.
- Carter, W.P.L., 1990. A detailed mechanism for the gas-phase atmospheric reactions of organic compounds. *Atmos. Environ.* 24, 481–518.
- Carter, W.P.L., 2000. Implementation of the SAPRC99 Chemical Mechanism into the Models-3 Framework. Report to the U.S. EPA, Statewide Air Pollution Research Center, University of California, Riverside, CA, USA.
- Chen, F., Dudhia, J., 2001. Coupling an advanced land surface–hydrology model with the Penn State NCAR MM5 modeling system. Part I: model implementation and sensitivity. *Mon. Weather Rev.* 129, 569–585.
- Chen, S.H., Sun, W.Y., 2002. A one dimensional time dependent cloud model. *J. Meteorol. Soc. Jpn.* 80, 99–118. <http://dx.doi.org/10.2151/jmsj.80.99>.
- Chen, D.S., Cheng, S.Y., Liu, L., Chen, T., Guo, X.R., 2007. An integrated MM5-CMAQ modeling approach for assessing trans-boundary PM₁₀ contribution to the host city of 2008 Olympic summer games-Beijing, China. *Atmos. Environ.* 41, 1237–1250.
- Chen, D.S., Cheng, S.Y., Liu, L., Lei, T., Guo, X.R., Zhao, X.Y., 2008. Assessment of the integrated ARPS-CMAQ modeling system through simulating PM₁₀ concentration in Beijing, China. *Environ. Eng. Sci.* 25 (2), 191–206.
- Chen, S.Y., Huang, J.P., Zhao, C., Qian, Y., Leung, L.R., Yang, B., 2013. Modeling the transport and radiative forcing of Taklimakan dust over the Tibetan Plateau: a case study in the summer of 2006. *J. Geophys. Res.* 118, 797–812. <http://dx.doi.org/10.1002/jgrd.50122>.
- Chou, M.D., Suarez, M.J., Ho, C.H., Yan, M.M.H., Lee, K.T., 1998. Parameterizations for cloud overlapping and shortwave single scattering properties for use in general circulation and cloud ensemble models. *J. Clim.* 11, 202–214.
- Ek, M.B., Mitchell, K.B., Lin, Y., Rogers, B., Grunmann, P., Koren, V., Gayno, G., Tarpley, J.D., 2003. Implementation of NOAA land surface model advances in the National Centers for Environmental Prediction operational mesoscale Eta model. *J. Geophys. Res.* 108 (D22), 8851. <http://dx.doi.org/10.1029/2002JD003296>.
- Emery, C., Tai, E., Yarwood, G., 2001. Enhanced Meteorological Modeling and Performance Evaluation for Two Texas Ozone Episodes. Final Report, The Texas Natural Resource Conservation Commission, 12118 Park 35 Circle Austin, Texas 78753, [online] Available from: <http://www.tceq.state.tx.us/assets/public/implementation/air/am/contracts/reports/mm/EnhancedMetModelingAndPerformanceEvaluation.pdf> (accessed 28.09.14.).
- Fast, J.D., Gustafson Jr., W.I., Easter, R.C., Zaveri, R.A., Barnard, J.C., Chapman, E.G., Grell, G.A., Peckham, S.E., 2006. Evolution of ozone, particulates, and aerosol direct radiative forcing on the vicinity of Houston using a fully coupled meteorology-chemistry-aerosol model. *J. Geophys. Res.* 111, D21305. <http://dx.doi.org/10.1029/2005JD006721>.
- Fu, J.S., Streets, D.G., Jang, C.J., Hao, J.M., He, K.B., Wang, L.T., Zhang, Q., 2009. Modeling regional/urban ozone and particulate matter in Beijing, China. *J. Air Waste Manage. Assoc.* 59, 37–44.
- Gao, Y., Zhang, M.G., 2012. Sensitivity analysis of surface ozone to emission controls in Beijing and its neighboring area during the 2008 Olympic Games. *J. Environ. Sci. China* 24 (1), 50–61.
- Garrett, T.J., Avey, L., Palmer, P.I., Stohl, A., Neuman, J.A., Brock, C.A., Ryerson, T.B., Holloway, J.S., 2006. Quantifying wet scavenging processes in aircraft observations of nitric acid and cloud condensation nuclei. *J. Geophys. Res.* 111, D23S51. <http://dx.doi.org/10.1029/2006JD007416>.
- Genoux, P., Chin, M., Tegen, I., Prospero, J., Holben, B., Dubovik, O., Lin, S.J., 2001. Sources and global distributions of dust aerosols simulated with the GOCART model. *J. Geophys. Res.* 106, 20,255–20,273.
- Gong, S.L., 2003. A parameterization of sea salt aerosol source function for sub and supermicron particles. *Glob. Biogeochem. Cy.* 17 (4), 1097. <http://dx.doi.org/10.1029/2003GB002079>.
- Grell, G.A., Devenyi, D., 2002. A generalized approach to parameterizing convection combining ensemble and data assimilation techniques. *Geophys. Res. Lett.* 29 (14), 1693. <http://dx.doi.org/10.1029/2002GL015311>.
- Grell, G.A., Peckham, S.E., Schmitz, R., McKeen, S.A., Frost, G., Skamarock, W.C., Eder, B., 2005. Fully coupled “online” chemistry within the WRF model. *Atmos. Environ.* 39, 6957–6975. <http://dx.doi.org/10.1016/j.atmosenv.2005.04.027>.
- Guenther, A., Karl, T., Harley, P., Wiedinmyer, C., Palmer, P.I., Geron, C., 2006. Estimates of global terrestrial isoprene emissions using MEGAN (Model of Emissions of Gases and Aerosols from Nature). *Atmos. Chem. Phys.* 6, 3181–3210.
- Han, S.Q., Feng, Y.C., Bian, H., Tie, X., Xie, Y.Y., Li, X.J., Sun, M.L., 2008. Numerical simulation of diurnal variation of major pollutants with WRF-Chem model in Tianjin, China. *Environ. Sci.* 28 (9), 828–832 (In Chinese).
- He, K.B., 2012. Multi-resolution Emission Inventory for China (MEIC): model framework and 1990–2010 anthropogenic emissions. In: Presented on the International Global Atmospheric Chemistry Conference, September 17–21, Beijing, China.
- Hong, S., Noh, Y., Dudhia, J., 2006. A new vertical diffusion package with an explicit treatment of entrainment processes. *Mon. Weather Rev.* 134, 2318–2341. <http://dx.doi.org/10.1175/MWR3199.1>.
- Huang, R.J., Zhang, Y.L., Bozzetti, C., Ho, K.F., Cao, J.J., Han, Y.M., Daellenbach, K.R., Slowik, J.G., Platt, S.M., Canonaco, F., Zotter, P., Wolf, F., Pieber, S., Bruns, E.A., Crippa, M., Ciarelli, G., Piazzalunga, A., Schwikowski, M., Abbaszade, G., Schnelle-Kreis, J., Zimmermann, R., An, Z., Szidat, S., Baltensperger, U., El Haddad, Imad, Prevot, A.S.H., 2014. High secondary aerosol contribution to particulate pollution during haze events in China. *Nature*. <http://dx.doi.org/10.1038/nature13774>.
- Iacono, M.J., Delamere, J.S., Mlawer, E.J., Shephard, M.W., Clough, S.A., Collins, W.D., 2008. Radiative forcing by longlived greenhouse gases: calculations with the AER radiative transfer models. *J. Geophys. Res.* 113, D13103. <http://dx.doi.org/10.1029/2008JD009944>.
- Ikeda, R., Kusaka, H., 2010. Proposing the simplification of the multilayer urban canopy model: intercomparison study of four models. *J. Appl. Meteor. Climatol.* 49, 902–919. <http://dx.doi.org/10.1175/2009JAMC2336.1>.
- Janjić, Z.I., 2001. Nonsingular Implementation of the Mellor–Yamada Level 2.5 Scheme in the NCEP Meso Model. NCEP Off. Note 437. Natl. Cent. for Environ. Predict., Camp Springs, Md, p. 61.
- Ji, D.S., Li, L., Wang, Y.S., Zhang, J.K., Cheng, M.T., Sun, Y., Liu, Z.R., Wang, L.L., Tang, G.Q., Hu, B., Chao, N., Wen, T.X., Miao, H.Y., 2014. The heaviest particulate air-pollution episodes occurred in northern China in January, 2013: insights gained from observation. *Atmos. Environ.* 92, 546–556.
- Jiang, J.K., Zhou, W., Cheng, Z., Wang, S.X., He, K.B., Hao, J.M., 2014. Particulate matter distributions in China during a Winter period with frequent pollution episodes (January 2013). *Aerosol Air Qual. Res.* <http://dx.doi.org/10.4209/aaqr.2014.04.0070> (in press).
- Kain, J.S., 2004. The Kain–Fritsch convective parameterization: an update. *J. Appl. Meteor.* 43, 170–181.
- Knote, C., Brunner, D., 2013. An advanced scheme for wet scavenging and liquid-phase chemistry in a regional online-coupled chemistry transport model. *Atmos. Chem. Phys.* 13, 1177–1192.
- Kusaka, H., Kimura, F., 2004. Thermal effects of urban canyon structure on the nocturnal heat island: numerical experiment using a mesoscale model coupled with an urban canopy model. *J. Appl. Meteor.* 43, 1899–1910.
- Li, N., Fu, T.M., Cao, J.J., Lee, S.C., Huang, X.F., He, L.Y., Ho, K.F., Fu, J.S., Lam, Y.F., 2013. Sources of secondary organic aerosols in the Pearl River Delta region in fall: contributions from the aqueous reactive uptake of dicarbonyls. *Atmos. Environ.* 76 (S1), 200–207.
- Li, M., Zhang, Q., Streets, D.G., et al., 2014. Mapping Asian anthropogenic emissions of non-methane volatile organic compounds to multiple chemical mechanisms. *Atmos. Chem. Phys.* 14, 5617–5638.
- Lim, K.S., Hong, S.Y., 2010. Development of an effective double moment cloud microphysics scheme with prognostic cloud condensation nuclei (CCN) for weather and climate models. *Mon. Wea. Rev.* 138, 1587–1612.
- Lin, Y.L., Farley, R.D., Orville, H.D., 1983. Bulk parameterization of the snow field in a cloud model. *J. Clim. Appl. Meteorol.* 22, 1065–1092.
- Lin, M., Holloway, T., Oki, T., Streets, D.G., Richter, A., 2009. Multi-scale model analysis of boundary layer ozone over East Asia. *Atmos. Chem. Phys.* 9, 3277–3301.
- Liu, X.H., Zhang, Y., Xing, J., Zhang, Q., Wang, K., Streets, D.G., Jang, C.J., Wang, W.X.,

- Hao, J.M., 2010. Understanding of regional air pollution over China using CMAQ, part II. Process analysis and sensitivity of ozone and particulate matter to precursor emissions. *Atmos. Environ.* 44, 3719–3727.
- Lu, X.Y., Tang, J., Zhang, J., Yue, J., Song, G.K., Hu, J.G., 2013. Annual Report on Analysis of Beijing Society-building. Social Science Academic Press, Beijing, China.
- Madronich, S., Flocke, S., 1998. The role of solar radiation in atmospheric chemistry. In: Boule, P. (Ed.), *Handbook of Environmental Chemistry*. Springer-Verlag, Heidelberg, p. 126.
- Misenis, C., Zhang, Y., 2010. An examination of sensitivity of WRF/Chem predictions to physical parameterizations, horizontal grid spacing, and nesting options. *Atmos. Res.* 97, 315–334.
- Mlawer, E.J., Taubman, S.J., Brown, P.D., Iacono, M.J., Clough, S.A., 1997. Radiative transfer for inhomogeneous atmospheres: RRTM, a validated correlated k model for the longwave. *J. Geophys. Res.* 102 (D14), 16,663–16,682. <http://dx.doi.org/10.1029/97JD00237>.
- Monin, A.S., Obukhov, A.M., 1954. Basic laws of turbulent mixing in the surface layer of the atmosphere [in Russian] *Tr. Geophys. Inst. Akad. Nauk. SSSR* 24 (151), 163–187.
- Morrison, H., Thompson, G., Tatarskii, V., 2009. Impact of cloud microphysics on the development of trailing stratiform precipitation in a simulated squall line: comparison of one and two moment schemes. *Mon. Wea. Rev.* 137, 991–1007. <http://dx.doi.org/10.1175/2008MWR2556.1>.
- NBS, 2013. China Statistical Yearbook 2013. China Statistical Press, Beijing, China.
- NCAR, 2013. Advanced Research WRF (ARW) Version 3.5 Modeling System User's Guide. NCAR, USA.
- Peckham, S.E., Grell, G.A., McKeen, S.A., Ahmadov, R., Brar, M., Pfister, G., Wiedinmyer, C., Fast, J.D., Gustafson, W.I., Ghan, S.J., Zaveri, R., Easter, R.C., Barnard, J., Chapman, E., Hewson, M., Schmitz, R., Salzmann, M., Beck, V., Freitas, S., 2013. WRF/Chem Version 3.5 User's Guide. NOAA, USA.
- Pleim, J.E., Xiu, A., 1995. Development and testing of a surface flux and planetary boundary layer model for application in mesoscale models. *J. Appl. Meteorol.* 34, 16–32.
- Pleim, J.E., 2006. A simple, efficient solution of flux profile relationships in the atmospheric surface layer. *J. Appl. Meteor. Clim.* 45, 341–347.
- Pleim, J.E., 2007. A combined local and nonlocal closure model for the atmospheric boundary layer. Part I: model description and testing. *J. Appl. Meteor. Climatol.* 46, 1383–1395.
- Saide, P.E., Spak, S.N., Carmichael, G.R., Mena-Carrasco, M.A., Yang, Q., Howell, S., Leon, D.C., Snider, J.R., Bandy, A.R., Collett, J.L., Benedict, K.B., de Szoeko, S.P., Hawkins, L.N., Allen, G., Crawford, L., Crosier, J., Springston, S.R., 2012. Evaluating WRF-Chem aerosol indirect effects in Southeast Pacific marine stratocumulus during VOCALS-REx. *Atmos. Chem. Phys.* 12, 3045–3064.
- Shrivastava, M., Fast, J., Easter, R., Gustafson Jr., W.I., Zaveri, R.A., Jimenez, J.L., Saide, P., Hodzic, A., 2011. Modeling organic aerosols in a megacity: comparison of simple and complex representations of the volatility basis set approach. *Atmos. Chem. Phys.* 11, 6639–6662. <http://dx.doi.org/10.5194/acp1166392011>.
- Situ, S., Guenther, A., Wang, X., Jiang, X., Turnipseed, A., Wu, Z., Bai, J., Wang, X., 2013. Impacts of seasonal and regional variability in biogenic VOC emissions on surface ozone in the Pearl River delta region, China. *Atmos. Chem. Phys.* 13, 11803–11817.
- Streets, D.G., Fu, J.S., Jang, C.J., Hao, J.M., He, K.B., Tang, X.Y., Zhang, Y.H., Wang, Z.F., Li, Z.P., Zhang, Q., Wang, L.T., Wang, B.Y., Yu, C., 2007. Air quality during the 2008 Beijing Olympic Games. *Atmos. Environ.* 41, 480–492.
- Tesche, T.W., McNally, D.E., Emery, C.A., Tai, E., 2001. Evaluation of the MM5 Model Over the Midwestern U.S. for Three 8-hour Oxidant Episodes. Alpine Geophysics, LLC, Ft. Wright, KY, and ENVIRON International Corp., Novato, CA.
- Tie, X.X., Geng, F.H., Peng, L., Gao, W., Zhao, C.S., 2009. Measurement and modeling of O₃ variability in Shanghai, China: application of the WRF-Chem model. *Atmos. Environ.* 43 (28), 4289–4302.
- Tie, X.X., Geng, F., Guenther, A., Cao, J., Greenberg, J., Zhang, R., Apel, E., Li, G., Weinheimer, W., Chen, J., Cai, C., 2013. Megacity impacts on regional ozone formation: observations and WRF-Chem modeling for the MIRAGE-Shanghai field campaign. *Atmos. Chem. Phys.* 13, 5655–5669.
- Tonnesen, G.S., Dennis, R.L., 2000a. Analysis of radical propagation efficiency to assess ozone sensitivity to hydrocarbons and NO_x 1. Local indicators of instantaneous odd oxygen production sensitivity. *J. Geophys. Res.* 105 (D7), 9213–9225.
- Tonnesen, G.S., Dennis, R.L., 2000b. Analysis of radical propagation efficiency to assess ozone sensitivity to hydrocarbons and NO_x 2. Long-lived species as indicators of ozone concentration sensitivity. *J. Geophys. Res.* 105 (D7), 9227–9241.
- Tuccella, P., Curci, G., Visconti, G., Bessagnet, B., Menut, L., Park, R.J., 2012. Modeling of gas and aerosol with WRF/Chem over Europe: evaluation and sensitivity study. *J. Geophys. Res.* 117, D03303. <http://dx.doi.org/10.1029/2011JD016302>.
- U.S. EPA, 2007. Guidance on the Use of Models and Other Analyses for Demonstrating Attainment of Air Quality Goals for Ozone, PM_{2.5}, and Regional Haze. Office of Air and Radiation/Office of Air Quality Planning and Standards, Research Triangle Park, NC, USA.
- Wang, L.T., Hao, J.M., He, K.B., Wang, S.X., Li, J., Zhang, Q., Streets, D.G., Fu, J.S., Jang, C.J., Takekawa, H., Chatani, S., 2008. A modeling study of coarse particulate matter pollution in Beijing: regional source contributions and control implications for the 2008 Summer Olympics. *J. Air Waste Manage. Assoc.* 58, 1057–1069. <http://dx.doi.org/10.3155/1047-3289.58.8.1057>.
- Wang, K., Zhang, Y., Jang, C.J., Phillips, S., Wang, B.Y., 2009. Modeling study of intercontinental air pollution transport over the trans-pacific region in 2001 using the community multiscale air quality (CMAQ) modeling system. *J. Geophys. Res.* 114 (D4), D04307. <http://dx.doi.org/10.1029/2008JD010807>.
- Wang, S.X., Xing, J., Jang, C.J., Zhu, Y., Fu, J.S., Hao, J.M., 2011. Impact assessment of ammonia emissions on inorganic aerosols in east China using response surface modeling technique. *Environ. Sci. Tech.* 45, 9293–9300.
- Wang, J.D., Wang, S.X., Jiang, J.K., Ding, A.J., Zheng, M., Zhao, B., Wong, D.C., Zhou, W., Zheng, G.J., Wang, L., Pleim, J.E., Hao, J.M., 2014a. Impact of aerosol–meteorology interactions on fine particle pollution during China's severe haze episode in January 2013. *Environ. Res. Lett.* 9, 094002. <http://dx.doi.org/10.1088/1748-9326/9/9/094002>.
- Wang, L.T., Wei, Z., Yang, J., Zhang, Y., Zhang, F.F., Su, J., Meng, C.C., Zhang, Q., 2014b. The 2013 severe haze over southern Hebei, China: model evaluation, source apportionment, and policy implications. *Atmos. Chem. Phys.* 14, 3151–3173. <http://dx.doi.org/10.5194/acp-14-3151-2014>.
- Wang, Y.S., Yao, L., Wang, L.L., Liu, Z.R., Ji, D.S., Tang, G.Q., Zhang, J.K., Sun, Y., Hu, B., Xin, J.Y., 2014c. Mechanism for the formation of the January 2013 heavy haze pollution episode over central and eastern China. *Sci. China Earth Sci.* 57 (1), 14–25.
- Wei, Z., Yang, J., Wang, L.T., Wei, W., Zhang, F.F., Su, J., 2014. Characteristics of the severe haze episode in Handan city in January, 2013. *Acta Sci. Circumst.* 34 (5), 1118–1124 (in Chinese).
- Wu, L.T., Su, H., Jiang, J.H., 2013. Regional simulation of aerosol impacts on precipitation during the East Asian summer monsoon. *J. Geophys. Res.* 118, 6454–6467. <http://dx.doi.org/10.1002/jgrd.50527>.
- Xing, J., Zhang, Y., Wang, S.X., Liu, X.H., Cheng, S.H., Zhang, Q., Chen, Y.S., Streets, D.G., Jang, C.J., Hao, J.M., Wang, W.X., 2011. Modeling study on the air quality impacts from emission reductions and a typical meteorological conditions during the 2008 Beijing Olympics. *Atmos. Environ.* 45, 1786–1798.
- Xiu, A., Pleim, J.E., 2001. Development of a land surface model, part I: application in a mesoscale meteorological model. *J. Appl. Meteorol.* 40, 192–209.
- Yan, R.S., 2013. Simulation and Analysis of Wintertime Typical Particulate Matter Pollution Episode in Beijing. Master thesis. Nanjing University of Information Science and Technology, Nanjing, China (in Chinese).
- Zaveri, R.A., Easter, R.C., Fast, J.D., Peters, L.K., 2008. Model for simulating aerosol interactions and chemistry (MOSAIC). *J. Geophys. Res.* 113, D13204. <http://dx.doi.org/10.1029/2007JD008792>.
- Zhang, Y., Liu, P., Pun, B., Seigneur, C., 2006. A comprehensive performance evaluation of MM5-CMAQ for the Summer 1999 Southern Oxidants Study episode-Part I: evaluation protocols, databases, and meteorological predictions. *Atmos. Environ.* 40, 4825–4838.
- Zhang, Y., 2008. Online coupled meteorology and chemistry models: history, current status, and Outlook. *Atmos. Chem. Phys.* 8, 2895–2932.
- Zhang, Q., Streets, D.G., Carmichael, G.R., He, K.B., Huo, H., Kannari, A., Klimont, Z., Park, I.S., Reddy, S., Fu, J.S., Chen, D., Duan, L., Lei, Y., Wang, L.T., Yao, Z.L., 2009a. Asian emissions in 2006 for the NASA INTEX-B mission. *Atmos. Chem. Phys.* 9, 5131–5153.
- Zhang, Y., Wen, X.Y., Wang, K., Vijayaraghavan, K., Jacobson, M.Z., 2009b. Probing into regional O₃ and particulate matter pollution in the United States: 2. An examination of formation mechanisms through a process analysis technique and sensitivity study. *J. Geophys. Res.* 114, D22305. <http://dx.doi.org/10.1029/2009JD011900>.
- Zhang, Y., Wen, X.Y., Jang, C.J., 2010a. Simulating chemistry-aerosol-cloud-radiation-climate feedbacks over the continental U.S. using the online-coupled Weather Research Forecasting Model with Chemistry (WRF/Chem). *Atmos. Environ.* 44, 3568–3582.
- Zhang, Y., Liu, X.H., Olsen, K.M., et al., 2010b. Responses of future air quality to emission controls over North Carolina, Part II: Analyses of future-year predictions and their policy implications. *Atmos. Environ.* 44, 2767–2779.
- Zhang, Y., Bocquet, M., Mallet, V., Seigneur, C., Baklanov, A., 2012a. Real-time air quality forecasting, part I: history, techniques, and current status. *Atmos. Environ.* 60, 632–655.
- Zhang, Y., Chen, Y.S., Sarwar, G., Schere, K., 2012b. Impact of gas-phase mechanisms on Weather Research Forecasting Model with Chemistry (WRF/Chem) predictions: mechanism implementation and comparative evaluation. *J. Geophys. Res.* 117, D01301. <http://dx.doi.org/10.1029/2011JD015775>.
- Zhang, Y., Karamchandani, P., Glotfelty, T., Streets, D.G., Grell, G., Nenes, A., Yu, F.Q., Bannartz, R., 2012c. Development and initial application of the global-through-urban Weather Research and Forecasting Model with Chemistry (GU-WRF/Chem). *J. Geophys. Res.* 117, D20206. <http://dx.doi.org/10.1029/2012JD017966>.
- Zhang, Y., Sartelet, K., Zhu, S., Wang, W., Wu, S.Y., Zhang, X., Wang, K., Trans, P., Seigneur, C., Wang, Z.F., 2013. Application of WRF/Chem-MADRID and WRF/Polyphemus in Europe – Part 2: evaluation of chemical concentrations and sensitivity simulations. *Atmos. Chem. Phys.* 13, 6845–6875.
- Zhao, B., Wang, S.X., Wang, J.D., Fu, J.S., Liu, T.H., Xu, J.Y., Fu, X., Hao, J.M., 2013. Impact of national NO_x and SO₂ control policies on particulate matter pollution in China. *Atmos. Environ.* 77, 453–463.
- Zheng, G.J., Duan, F.K., Ma, Y.L., Cheng, Y., Zheng, B., Zhang, Q., Huang, T., Kimoto, T., Chang, D., Su, H., Pöschl, U., Cheng, Y.F., He, K.B., 2014. Exploring the severe winter haze in Beijing. *Atmos. Chem. Phys. Discuss.* 14, 17907–17942.
- Zhou, Y., Fu, J.S., Zhuang, G.S., Levy, J.I., 2010. Risk-based prioritization among air pollution control strategies in the Yangtze River Delta, China. *Environ. Health Perspect.* 118 (9), 1204–1210.
- Zhou, Y., Cheng, S.Y., Liu, L., Chen, D.S., 2012. A coupled MM5-CMAQ modeling system for assessing effects of restriction measures on PM₁₀ pollution in Olympic city of Beijing, China. *J. Environ. Inform.* 19 (2), 120–127.